Arabidopsis arenosa influences its microbiome as a serpentine soil adaptation strategy

Anita Bollmann-Giolai[1,2], Michael Giolai[1,3], Mellieha Allen[4], Darren Heavens[5], Veronika Lipánová[6], Mark Alston[5], James Brown[1], Matthew D. Clark[7], Paulina Flis[8], Filip Kolář[9], Levi Yant[8], Jacob Malone[1,10]

1) John Innes Centre, Norwich Research Park, Norwich NR4 7UH, United Kingdom

2) Max Planck Institute for Biology, Tübingen, 72076, Germany

3) Research Centre for Ecological Change, Organismal and Evolutionary Biology Research Program, Faculty of Biological and Environmental Sciences, University of Helsinki, Finland

4) Royal Botanic Gardens, Kew, Kew Green, Richmond, Surrey, TW9 3AE, United Kingdom

5) Earlham Institute, Norwich Research Park, Norwich, NR4 7UZ, United Kingdom

6) Institute of Integrative Biology, ETH Zurich, Universitätstrasse 16, 8092 Zürich, Switzerland

7) Natural History Museum, London, SW7 5BD, United Kingdom

8) University of Nottingham, Nottingham NG7 2RD, UK

9) Institute of Botany, Czech Academy of Sciences, Průhonice 252 43, Czech Republic

10) School of Biological Sciences, University of East Anglia, Norwich NR4 7TJ, United Kingdom

Correspondence

All correspondence should be issued to: jacob.malone@jic.ac.uk.

Competing Interests

The authors declare no competing interests.

Abstract

There is growing evidence that microbes can facilitate plant growth in metal-rich soils. However, our current understanding of how plants recruit their microbiomes under abiotic stress remains incomplete. Serpentine soils are elementally skewed, with high concentrations of magnesium and nickel, often accompanied by other heavy metals, which can limit calcium availability and present unique challenges to plant growth. These soils are also nutrient-poor, prone to erosion, and have low water-holding capacity. To date, the mechanisms by which plants adapt to serpentine soils remain

poorly understood and the role of plant-associated microbiomes in this process has not been described. Here, we focus on *Arabidopsis arenosa* populations adapted to serpentine conditions and investigate their bacterial and fungal microbiomes to better understand the role of plant-associated microbes in serpentine adaptation. We show that serpentine soils harbour distinct plant-associated microbiomes across different plant niches and that the plant genetic background plays a key role in shaping microbial community composition. Finally, we identify serpentine-specific bacterial and fungal variants that may contribute to plant adaptation under these challenging soil conditions.

Introduction

There is growing evidence suggesting that microbes facilitate plant growth in heavy metal rich soils[1–7]. The plant microbiome influences growth, development and health[8–20]. However, knowledge of how plants attract their microbiome under abiotic stress conditions and the consequences of this for stress survival, is incomplete[9,21,22]. Stress responses such as root morphology or exudation some of can influence plant-microbe interactions[6,21–23]. Plants from highly metal-contaminated sites show distinct microbiomes compared to non-contaminated sites[24,25]. Microorganisms can be used to bioremediate contaminated mining sites[26]. A recent study describes serpentine-derived microbes improving seedling survival in serpentine soils[27].

Serpentine soils are naturally toxic to plants, globally distributed and derived from ferromagnesium-rich mantle rocks[28,29]. They are the most abundant heavy-metal soils, with elevated nickel, chromium, cobalt and high magnesium, causing low calcium/magnesium ratios and thus magnesium toxicity for plants[28–30]. Serpentine soils often lack essential nutrients[29], are often rocky, erosion- and drought-prone, with a shallow soil profile with low water-holding capacity[28,29,31]. Such high-stress conditions can have a significant impact on the ecosystem, influencing vegetation composition and leading to a high proportion of endemic species[28,29,31]. Therefore, plants growing on these sites must tolerate both drought and heavy-metals[29,31].

Serpentine site plants and their adaptation to those conditions have been studied since the 1950s[32–38]. However, in addition to the plants' inherent capacity to adapt to abiotic and biotic stress, they further rely on their microbiome to enable growth and survival in stressful conditions[8,9,39,40].

To study plant serpentine adaptation we use an autotetraploid lineage of *A. arenosa*, an outcrosser of the *Arabidopsis* genus, distributed in central and northern Europe as a model plant[33,41,42]. *A. arenosa* repeatedly adapted to serpentine soils and also grows on mining sites[41]. The plant is a facultative excluding metallophyte and also grows on non- contaminated soils[31,43,44]. For serpentine *A. arenosa* populations, genomics data suggests that genes related to the cation transport or chemical

homeostasis are under positive selection[33,37] while a reciprocal transplant experiment documented the fitness advantage of originally serpentine plants in their native substrate[37,38]. Thus, replicated populations, fitness phenotypes and genomic selection signatures make *A. arenosa* to a suitable for serpentine adaptation[45].

Both environmental and genetic factors influence microbiome formation, but their relative roles under abiotic stress remain unclear. To address this, we examine microbiomes of serpentine and non-serpentine *A. arenosa* populations and assess the relative contributions of environment and plant genome to microbial recruitment We select populations in Austria and the Czech Republic previously characterised for serpentine adaptation[33,37]. Over two seasons, we sampled three serpentine and three nearby non-serpentine sites for microbiomes from different plant niches (i.e., leaf, root, rhizosphere and bulk soil). We also conducted a common garden transplant experiment with all six populations to test genetic effects on microbiome assemblage in both soils. We show that serpentine soils shape microbiomes across niches and that plant genetic background is a major driver of composition. We further identify serpentine-specific bacterial and fungal amplicon sequence variants (ASVs) potentially facilitating adaptation to these challenging soils.

Results

Soil ion profiles distinguish serpentine and non-serpentine sites

Serpentine soils are characterized by drought conditions, low nutrient availability, high concentrations of heavy metals and magnesium, and low levels of calcium[46,47]. Magnesium, although being essential to plant growth, has been described to exacerbate the toxicity of other ions, including heavy metals, particularly under low calcium availability[29,48,49]. As a consequence, together with heavy metals, this enhances the toxicity of serpentine soils for plants[50]. Not many plant species grow in such challenging conditions, but *A. arenosa* populations have been previously described to show local adaptation to serpentine soils[37,38,45] (**Fig. 1A**).

We selected three pairs of populations established in either serpentine or non-serpentine soils, which are growing in spatial proximity in Austria and the Czech Republic (**Fig. 1A**). To confirm the soil ion profiles of the selected sites we collected soil material along with microbiome sampling and analysed the ion composition data of all sites (**Fig. 1B-E, Extended Data File 1**). Principal component analysis (PCA) of soil ion composition showed that that serpentine and non-serpentine soils separated well along PC1, which explained 43.2 % of variance (**Fig. 1B**). Magnesium, calcium and rubidium as well as the heavy metals nickel, chromium and cobalt contributed most to the separation (**Fig. 1C**). The magnesium concentration showed the strongest association with serpentine soils along PC1. We also

analysed the Ca/Mg ratio and found that the ratio was consistently lower in serpentine than non-serpentine soils (**Fig. 1C-E**, **Extended Data File 1**). This pattern agrees with previously described characteristics of serpentine soils[32].

Microbiome community structure across serpentine and non-serpentine niches

We collected bulk soil (adjacent to plants), rhizosphere, root and leaf material in spring and fall 2018 from five plants per population. We constructed and sequenced 16S and ITS Illumina amplicon libraries and assigned ASVs[23,51], removing ASVs below a total relative abundance of 0.1%. We performed a redundancy analysis (RDA) to assess community structure across all niches using genus-level taxonomic resolution (**Fig. 2, Extended Data File 2**). Here, we observed stronger niche differentiation in bacterial communities (**Fig. 2A, Extended Data File 2**) compared to fungal communities (**Fig. 2C, Extended Data File 2**). In both bacteria and fungi, leaf-associated communities were clearly distinct from those in bulk soil, rhizosphere, and roots (**Extended Data File 2**).

ASVs were grouped by phylum and illustrated in bar plots to understand bacterial and fungal microbiome composition across populations and seasons (**Fig. 2B,D**). Bar plots indicated that the phylum-level composition of bacterial and fungal communities was largely similar between serpentine and non-serpentine sites, but showed niche specific differences between bacteria and fungi. Multiple bacterial phyla were present across all four niches, whereas fungal communities were dominated by few highly abundant phyla. This aligns with previous findings that bacterial niches exhibit greater diversity and niche differentiation compared to fungi[52]. For bacteria, 11 and 13 phyla were detected in bulk soil and rhizosphere compared to 8 in roots and 5 in leaves (**Fig. 2B**). In the bulk soil compartment Cyanobacteria, Proteobacteria, Actinobacteria, Verrumicrobiota and Acidobacteriota shared equal relative abundances (22.71 % - 16.12 % of assigned ASVs respectively). The same pattern was observed for the rhizosphere, with some changes in abundances and an increase of Cyanobacteria from 22.71 % to 31.35 % of assigned ASVs. Roots were dominated by Actinobacteria (44.19 %) and Proteobacteria (31.59 %), whereas leaves were highly enriched in Proteobacteria with 78.22 % of assigned ASVs (**Extended Data File 3**). This indicates potential niche specific shifts and composition of bacterial taxa from bulk soil to the rhizosphere, as well as roots to leaves. Fungal communities exhibited less clear niche differences (**Fig. 2D**). Bulk soil and rhizosphere contained 3 and 4 phyla while roots and leaves contained 3 and 2 phyla respectively. Ascomycota and Basidiomycota together accounted for the majority of relative abundances across all niches. Ascomycota enriched for an average percentage of 58.74 %, 56.16 %, 71.37 % and 60.26 % from bulk soil, rhizosphere, roots to leaves. For Basidiomycota these loads were 39.67 %, 41.55 %, 27.2 % and 39.24 % respectively

124 (**Extended Data File 3**). The observation of differences in microbial composition between niches of
125 serpentine and non-serpentine plants agrees with previous findings by Botha *et al.*[53].

126 **Differential abundance analysis reveals serpentine-specific enrichment of microbial taxa**

127 We hypothesised that functional effects of a potential microbiome facilitated serpentine adaptation
128 likely occur at a finer taxonomic resolution than the phylum level (e.g., genus or species)[53,54].

129 Therefore, we tested whether individual ASVs influenced differences in community composition by
130 examining their occurrence across plants and populations: ASVs present in all populations were
131 considered conserved, those found in two of three populations were classed as shared, and those
132 restricted to a single population as unique (**Fig. 3A**). Analyses were performed for each niche, for
133 serpentine and non-serpentine sites, and for bacterial and fungal communities. Across 14,021
134 bacterial and 5,672 fungal ASVs we found that most bacterial and fungal ASVs were unique to
135 individual populations (**Fig. 3A, Extended Data File 4**). A fraction of 1.10 % – 9.17 % of serpentine
136 bacterial ASVs and 7.49 % - 9.51 % for serpentine fungal ASVs was conserved across niches. For non-
137 serpentine niches these numbers were lower with 0.31 % - 7.48 % and 3.16 % - 8.52 % for bacterial
138 and fungal ASVs across niches respectively. We observed the highest number of conserved ASVs for
139 fungal serpentine microbiomes (**Fig. 3A, Extended Data File 4**). Despite the large number of ASVs that
140 were unique to individual populations, the results indicate that plants growing on serpentines harbour
141 a conserved subset within their microbial communities that potentially contributes to serpentine
142 adaptation[24,25,53].

143 To test whether these patterns reflect statistically significant compositional shifts between
144 serpentines and non-serpentines, we performed differential abundance analysis using the
145 microbiomeMarker package[55] (**Fig. 3B**). A total of 13,895 bacterial and 5,618 fungal ASVs met
146 prevalence criteria[55]. Of these we found that 13.74 % of bacterial and 22.59 % of fungal ASVs were
147 statistically significantly enriched (**Extended Data File 5, Extended Data File 6**). Whereas 2.84 % of
148 13.74 % of bacterial ASVs across all niches enriched for serpentines. For the fungi this pattern was the
149 other way around and the majority of ASVs enriched for serpentines with 16.02 % of 22.59 %. These
150 results indicate that fine-scale taxonomic shifts accompany the previously observed broader
151 community differences. We next analysed the genera to which serpentine-enriched ASVs belonged.
152 For each genus, we counted the number of ASVs and calculated the $\log_2$-fold-ratio of serpentine to
153 non-serpentine ASVs. (**Extended Data File 5, Extended Data File 6**). For bacteria in bulk soil, no genus
154 showed a substantially higher number of ASVs in serpentine sites. In the serpentine rhizosphere,
155 *Candidatus Udaeobacter* was the most enriched genus with 47 ASVs compared to none in non-
156 serpentine sites, followed by *Vicinamibacterales* with 16 vs. 0 ASVs. In roots, genera generally had

157 lower ASV numbers, with *Streptomyces* showing 4 vs. 0 ASVs compared to serpentine sites. In leaves,
158 *Hymenobacter* and *Methylobacterium–Methylorubrum* counted more ASVs for serpentines, with 45
159 vs. 0 and 25 versus 0 ASVs to non-serpentines, respectively. For fungi, *Mytilinidion* (19 vs. 0), *Knufia*
160 and *Russula* (both 13 vs. 0) were most abundant in bulk soil, while no genera were notably enriched
161 in the rhizosphere. In roots, *Penicillium* (7 vs. 0), *Knufia*, *Sebacina,* and *Tomentella* (all 4 vs. 0) were
162 enriched, and in leaves, *Fellozyma* was observed with 4 vs. 0 ASVs compared to non-serpentines
163 (**Extended Data File 7**). Consolidating known literature about these genera we found commonalities
164 among bacteria and fungi that potentially contribute to microbiome mediated serpentine adaptation.
165 I.e., *Streptomyces* and *Methylobacterium–Methylorubrum* bacterial genera have been described to be
166 beneficial for plant performance and growth[56–58]. *Sebacinales* fungi are potential plant growth
167 promoting endophytes[59]. *Penicillium* fungi are described as decomposers of organic materials[60], and
168 *Tomentella* and *Russula* have been recognised as ectomycorrhizal fungi that are important in nutrient
169 cycling[61,62]. Hence, bacterial and fungal genera could together contribute to serpentine adaptation by
170 facilitating nutrient availability and promoting plant growth in serpentines. This agrees with previous
171 findings where serpentine plants have been described to associate with arbuscular mycorrhizal
172 assemblages[63].

173 **Serpentine microbiomes are better retained by native plants under reverse-transplant conditions**

174 Previous studies have shown that plant genotypes can influence the composition of their associated
175 microbiomes[64–67]. However, environmental factors also significantly impact microbial community
176 composition and environmental stressors can influence the recruitment of specific microbial taxa that
177 may aid in plant adaptation[68]. It remains unclear to what extent plants actively recruit microbes or
178 whether observed effects are environmentally driven.

179 To examine potential recruitment effects, we predicted that non-serpentine genotypes, which are not
180 typically adapted to serpentine soils[38], would exhibit different responses compared to serpentine
181 genotypes under serpentine conditions. To test this, we performed a reciprocal transplant experiment
182 in which serpentine and non-serpentine populations were grown in both serpentine and non-
183 serpentine soils. As in the field experiment, we collected five plants for each condition, performed 16S
184 and ITS Illumina sequencing and called ASVs[69]. We then compared ASV abundances of serpentine and
185 non-serpentine populations grown in their native soil type with those in the transplanted (i.e., non-
186 native) soil using Bray-Curtis similarity (**Fig. 4A,B**). We observed that microbiomes between native and
187 non-native conditions differed substantially, yet not completely, between populations. Fungal
188 microbiomes were more similar than bacterial microbiomes in the bulk soil and the root
189 compartments (**Fig. 4C, Extended Data File 8**). To test whether serpentine and non-serpentine plants

190 recruit similar microbiomes under serpentine conditions, we compared the $\log_2$ fold-changes of ASVs
191 observed in the field with those measured in the transplant experiment, focusing on serpentine-to-
192 non-serpentine enrichment. Log_2 fold-change values were compared using Spearman's rank
193 correlation coefficients (**Fig. 4C**). The analyses showed that $\log_2$ fold-changes in serpentine plants from
194 the transplant experiment agreed more closely with field data and preserved the patterns observed
195 in the field better than those of non-serpentine plants. For serpentine plants, Spearman correlation
196 coefficients with the field data were 0.71, 0.66, and 0.59 for bulk soil, rhizosphere, and root,
197 respectively (all statistically significant: $p \leq 2\text{x}10^{-16}$, $p = 5\text{x}10^{-3}$, and $p = 5\text{x}10^{-4}$). For non-serpentine
198 plants, correlations were weaker with 0.62 and 0.46 for bulk soil and root (bulk soil $p = 1.8\text{x}10^{-12}$, root
199 $p = 1.9\text{x}10^{-2}$). These results indicate that serpentine plants maintained a microbiome that more closely
200 resembles the field serpentine gradient than non-serpentine plants. No statistically significant
201 correlations were observed in leaves, which potentially reflects aboveground effects of growth under
202 controlled conditions rather than patterns present in the field.

203 We hypothesised that ASVs with a potential role in facilitating serpentine adaptation would be
204 statistically significantly serpentine-enriched in the field and the transplant data. We therefore
205 compared statistically significantly enriched bacterial and fungal ASVs from the field with those from
206 the transplant experiment (**Fig. 3D**). Overall, serpentine plants showed stronger overlap with field data
207 than non-serpentine plants. For bacteria, only three ASVs in bulk soil were serpentine-enriched in
208 populations of non-serpentine origin, whereas populations of serpentine origin showed greater
209 overlap, with six ASVs in bulk soil and nine in the rhizosphere. For fungi, the numbers were generally
210 higher. In serpentine-origin plants, we observed 90 overlapping ASVs in bulk soil, one in leaf, two in
211 the rhizosphere, and 24 in root. In contrast, non-serpentine-origin plants showed fewer overlaps, with
212 21 in bulk soil, none in leaf or rhizosphere, and 10 in root.

213 We found that fewer bacterial ASVs were enriched under serpentine conditions, whereas fungi
214 showed a greater number of consistently enriched ASVs, both in the field and in serpentine plants
215 during the transplant experiment. This overlap highlights fungal ASVs as potential contributors to
216 serpentine adaptation, particularly in belowground compartments such as bulk soil, rhizosphere, and
217 root. Among bacteria, only a single genus, *Candidatus Udaeobacter*, was enriched in both the
218 rhizosphere and bulk soil. In contrast, we identified 73 enriched associations with fungal taxa, 55 of
219 which could be assigned at the genus level (the remainder assigned at higher taxonomic ranks such as
220 phylum, order, or class). We also quantified the number of ASVs per genus and, consistent with the
221 field data, observed overlap with genera already detected in the natural serpentine community
222 (**Extended Data File 9**). For example, we identified six ASVs in *Penicillium*, three in *Russula*, and one
223 each in *Mytilinidion* and *Tomentella*. Consolidating literature further we also detected the fungal

224 genus *Exophiala*, which has been described to promote plant growth under nickel stress, a major
225 separator of serpentine conditions in our PCA[70] We also found the fungal genus *Phialocephala*, which
226 is a plant growth promoter by enabling nutrient availability[71]. Previous work has shown that
227 serpentine plants associate with distinct arbuscular mycorrhizal assemblages that may help mitigate
228 metal stress[63]. Our findings therefore indicate potential new fungal partners involved in serpentine
229 stress adaptation. Moreover, fungi associated with serpentine plants are often highly diverse and may
230 include specialized taxa that confer advantages to plants growing under serpentine conditions[72,73].

231 ***Plant genotype is a stronger factor shaping microbial communities, compared to the environment***

232 The extent to which plant-associated microbiomes are actively recruited by the host, shaped by
233 environmental conditions, or both remains unclear[74]. Considering enrichment patterns and
234 population differences between our field and transplant experiment, we concluded that microbiome
235 assembly results from a complex interplay between plant genotype and environmental factors, with
236 both likely contributing[75,76]. Disentangling the relative role of plant host and environment is essential
237 to determine whether microbiome-mediated stress adaptation is genetically encoded and thus
238 potentially subject to evolution or primarily environmentally induced.

239 To disentangle the effects of host genotype and environment on microbiome recruitment, we focused
240 on the statistically significant, differentially enriched ASVs identified in the field experiment. Genotype
241 data from populations revealed clear population separation in MDS analyses of k-mers from both
242 individual genome sequencing[37] (**Extended Data File 2**). We then applied generalized linear mixed
243 models (GLMMs) to test whether ASV abundances were explained by environment (serpentine vs.
244 non-serpentine), genotype (population), or their interaction. Model contributions were quantified
245 using R^2 values. Across all four niches, the combined effect of genotype and environment accounted
246 for the largest proportion of variance. Importantly, for both bacterial and fungal communities,
247 genotype-only models consistently explained more variance than environment-only models. These
248 results indicate that microbiome assembly is shaped by both host genotype and environment, with a
249 stronger contribution from genotype (**Fig. 5**). This pattern supports the idea that serpentine
250 adaptation reflects a long-term evolutionary process involving both plants and their associated
251 microbiomes.

252 **Discussion**

253 In this study, we conducted an in-depth examination of the microbiome communities associated with
254 *A. arenosa* plants growing in the challenging environment of serpentine soils. Serpentine soils impose
255 multiple simultaneous stresses, including low calcium-to-magnesium ratios, high heavy metal loads,

and nutrient deficiencies[32]. We show that serpentine soils differ from non-serpentine soils in their ionomic composition, most notably by a lower calcium-to-magnesium ratio. We further demonstrate that microbiomes of serpentine and non-serpentine plant populations differ in both bacterial and fungal composition across all tested compartments, from bulk soil to rhizosphere, roots, and leaves. In a reciprocal transplant experiment, exposing plants of serpentine and non-serpentine origin to both their native and non-native soils, we observe distinct microbial compositions depending on plant origin and soil type.

By carefully confirming field observations with a transplant experiment, we identify several ASVs and genera that can contribute to microbiome-mediated serpentine adaptation. Notably, many of the genera that we find as statistically significantly associated with serpentine soils are described to enhance either nutrient availability or to promote plant growth. This involves the coordinated contribution of both bacteria and fungi. Beneficial bacterial genera that we identify, such as *Streptomyces* and *Methylobacterium–Methylorubrum* enhance plant growth[56–58], while fungal taxa including *Sebacinales*, *Penicillium*, *Tomentella*, and *Russula* support nutrient cycling, organic matter decomposition, and soil nutrient acquisition[59–62]. Additionally, *Exophiala* and *Phialocephala* promote plant growth under nickel stress and improve nutrient availability[70,71]. Together, these microbes likely facilitate plant survival and growth under serpentine stress, complementing known associations with arbuscular mycorrhizal fungi[63]. Considering that serpentine soils are nutrient-poor and subject to heavy metal stress[32,46,47], the coordinated presence of microbial taxa that enhance nutrient availability, promote plant growth, and mitigate metal stress is likely crucial for plant survival under these conditions[9]. From an ecological and evolutionary perspective, these results are particularly impactful because they demonstrate a potential mechanism by which plants can extend their adaptive capacity through microbial partnerships.

In previous findings Konečná *et al.*[37] reported that *A. arenosa* exhibits an adaptive phenotype in serpentine soils, with this adaptation linked to 60 candidate genes, notably including the calcium channel *TPC1*. Whereas *TPC1* has not been connected to microbiome recruitment in detail[37], calcium channels play a role in plant signaling, microbe interactions[77]. In addition to confirming the importance of plant genetics in serpentine adaptation, we further show that the host genotype exerts a stronger effect than soil environment on the microbiome composition. This suggests that heritable plant traits influence microbial recruitment in ways that could reinforce adaptive phenotypes under stressful conditions. Such findings provide direct evidence supporting the holobiont concept, in which the plant and its microbiome function as an integrated adaptive unit[39]. Recognising the plant and its microbiome as an integrated adaptive unit opens new avenues for research and provides a roadmap for sustainable strategies to enhance plant health and productivity in challenging ecosystems[74,76,78,79].

290 In conclusion, our work highlights that microbial contributions to plant adaptation are both specific
291 and compartmentalized. The distinct patterns observed across niches demonstrate that adaptive
292 microbiomes are not uniform, but finely tuned to plant physiology and environmental context,
293 indicating tight plant–microbe co-evolution. This nuance is critical for understanding microbiome-
294 mediated stress adaptation, which cannot be inferred solely from bulk soil or aboveground sampling.

295 Our results bridge mechanistic understanding of plant adaptation with applied significance.
296 Serpentine soils can serve as a natural testbed to identify microbial taxa and plant genes that
297 contribute to stress resilience. Understanding which plant loci drive microbial recruitment could allow
298 future strategies to engineer crops that actively recruit beneficial microbes under nutrient-poor or
299 metal-contaminated conditions. This moves beyond correlative microbiome studies: it suggests a
300 pathway for predictive microbiome management, where plant genotype informs the assembly of
301 adaptive microbial consortia.

302 **Online Methods**

303 **Field sampling collection-strategy**

304 Serpentine and nearby, genetically close non-serpentine control populations were collected in the
305 Czech Republic and in Austria (**Fig. 1**). Populations N1 (49.734963, 15.174846, Vlastejovice) and S1
306 (49.683816, 15.133256, Borovsko) are located in the Czech Republic. Populations S2 (48.629930,
307 15.542567, Steinegg) and N2 (48.631497, 15.557237, Fuglau) are in Lower Austria, Austria and S3
308 (47.281679, 14.927647, Gulsen) and N3 (47.284170, 14.681940, Ingeringgraben) are in Styria, Austria.
309 The selected populations were sampled in spring 2018 and fall 2018. For each population different
310 tissues were sampled for their microbiomes: 1) leaf endophytes with closely associated epiphytes, 2)
311 root endophytes with closely associated epiphytes, 3) rhizosphere and nearby 4) bulk soil. As microbial
312 communities can change over time[80,81], we sampled all tissues at each time-point. For this, leaves,
313 roots, rhizosphere and bulk soil were collected in ten replicates. Additionally, soil and leaf material
314 were collected for comprehensive ionomic profiling at each time point.

315 **Field sample collection – microbiome samples**

316 All plant and soil material were collected using previously sterilised nitrile gloves and stored in 2 ml
317 Eppendorf safe-lock tubes (Eppendorf) in RNAlater (SIGMA-ALDRICH) to minimise microbial gDNA
318 degradation and community shifts. The sampled material was stored in a mobile refrigerator during
319 transportation where the material was stored at -80 °C until use for gDNA extraction.

320 **Field sample collection – microbiome samples of transplant experiment**

321 The transplant experiment is already published and described in[37,38]. In brief, to investigate adaptation
322 mechanisms of serpentine populations of *A. arenosa* to serpentine soils Konečná et al grew each
323 serpentine and its non-serpentine control population in a common garden set up in the experimental
324 garden of the Charles University, Prague (Czech Republic) over the growing season of 2019. Each
325 serpentine population was grown in its native serpentine soil and in the soil of its paired control non-
326 serpentine population and vice versa. Specifically, serpentine populations (S1, S2, S3) were grown in
327 their own serpentine soils (S1, S2, S3) as well as in the corresponding non-serpentine soils (N1, N2,
328 N3). Likewise, non-serpentine populations (N1, N2, N3) were grown in their own soils and in the paired
329 serpentine soils (S1, S2, S3). For example, population S1 was grown in its native serpentine S1 soil and
330 in the paired non-serpentine N1 soil, and population N1 was grown in its native N1 soil and the paired
331 serpentine S1 soil. In total 284 plants have been grown in total for the six populations, with 44-50
332 plants per population[37].

333 To investigate the role of the plant microbiome in serpentine soil adaptation, leaf, root and bulk-soil
334 material was collected for all populations grown in their natural and non-natural condition. All samples
335 had been collected in September 2019 with five replicates per plant tissue, population and treatment.
336 The collection and storing process was conducted as described above for microbiome samples.

337 **Field sample collection – ionomic profiling material**

338 Soil and leaf material were collected for ionomic elemental profiling. The soil was collected into 15 ml
339 conical tubes (Supplier Starlab (UK) Ltd). Leaves were collected into tea bags and stored in a box
340 containing silica gel to reduce moisture. The material was stored at room temperature until
341 preparation for elemental profiling.

342 **Ionomic material preparation**

343 The leaf and soil material were prepared for ionomic profiling by air-drying the soil for a minimum of
344 one week on the bench at room temperature and baking the leaves for three days at 60˚C until the
345 material was dry. The soil material was additionally sieved after baking to remove any debris. Leaf and
346 soil samples underwent elemental profiling with Inductively Coupled Plasma Mass Spectrometry (ICP-
347 MS) similar as described in[33,82]. Profiled elements were (names according to periodic table
348 annotations): Ca, Mg, Mn, Ni, Cr, Rb, Co and Fe.

349 **Ion profile analyses**

350 Ion concentration for elements of interest (namely Ca, Mg, Mn, Ni, Cr, Rb, Co and Fe) were visualised
351 using custom scripts in R-4.4.1 with the ggplot2-3.5.1 package[83]. Statistic differences between
352 serpentine and non-serpentine sites were tested using the stat_compare_means package of ggpubr-

353 0.6.0[84], specifying Wilcoxon rank-sum testing. The principal component analysis (PCA) was performed
354 using the default R-4.4.1 prcomp function. The graph of variables was visualised using the fviz_pca_var
355 function of factoextra-1.0.7[85] with default settings and the ggplot2-3.5.1[83] package in R-4.4.1.

356 **Map of populations**

357 Geographic coordinates of the serpentine and non-serpentine populations were converted into spatial
358 features using the sf-1.0 package in R-4.4.1, with WGS84 (EPSG:4326) as the reference coordinate
359 system. For visualization, a base map of Austria and Czechia was obtained from the rnaturalearth-
360 1.0.0 package at medium scale and used to display the location of populations[86] with ggplot2-3.5.1[83].

361 **Microbiome sample preparation**

362 Samples were stored in RNAlater[82,87–90]. Roots and leaves were transferred into a fresh 2 ml tube and
363 washed with 2 ml 0.1 M potassium phosphate pH 8.0 buffer with shaking at 200 rpm for 30 min.
364 Afterwards the root was transferred into a fresh 2 ml tube and supernatant was retained as the
365 rhizosphere sample. This step was repeated three times, with fresh buffer each time. Afterwards the
366 sample was vortexed twice for 30 seconds with fresh 2 ml 0.1 M potassium phosphate pH 8.0 buffer
367 and the root was transferred into a fresh 2 ml tube. The supernatant was added to the previously
368 collected supernatant. The combined supernatant was centrifuged for 10 min with 15,000 rcf and
369 room temperature. After removing the supernatant, the pellet was kept as a rhizosphere sample and
370 stored at -80˚C until further use. Leaf samples were washed with 2 ml 0.1 M potassium phosphate pH
371 8.0 buffer by vortexing twice for 10 sec. This step was repeated three times. The supernatant was
372 decanted, and leaves transferred into a fresh 2 ml tube and stored at -80˚C until further use.

373 **Microbiome gDNA extraction of field and transplant experiment samples**

374 The gDNA extraction for the field and common garden experiment was performed as described by
375 Bollmann-Giolai *et al.*[51] using 250 mg soil, before gDNA was purified in a 96-well format from 140 µl
376 supernatant using magnetic beads (Sera-Mag Carboxylate-Modified Magnetic Particles
377 (Hydrophophilic), GE Healthcare Life Sciences). The cleaned gDNA was transferred to a fresh 96 well
378 plate and stored at -20 ˚C until further use.

379 **Wet lab – Amplicon bacterial and fungal library construction**

380 Amplicon data was analysed as previously described[23,51]. In brief: The bacterial variable (V4) region of
381 the 16S rRNA gene and the fungal ITS1 region of the Internal Transcribed Spacer were targeted for
382 amplicon library construction using 16S 515 forward, 16S 806 reverse, ITS 1 forward and ITS2 reverse
383 primers adapted from Walters et al [91] (**Extended Data File 10**). Amplicon library construction was

384 performed using a two-step PCR protocol as previously described[23,51]: In a first PCR the 16S V4 and ITS
385 regions were targeted using gene specific primers, followed by custom dual indexing in a barcoding
386 PCR (**Extended Data File 10**). For the bacterial 16S V4 PCRs PNAs (peptide nucleic acid PCR clamps)
387 were included targeting plant mitochondria (mPNA) and chloroplast regions (cPNA)[92] in the first PCR
388 to minimise plant gene amplification. Library construction was conducted as previously described[23,51].
389 Briefly, the first PCR step was performed with three technical replicates using 3 ng gDNA. Samples
390 were then pooled and subjected to a 0.7x magnetic bead clean-up (MAGBIO) and eluted in 10 µl TE
391 buffer. The second PCR was conducted using the program for bacterial and fungal libraries previously
392 described[23,51].

393 The cleaned amplicon libraries were quantified using the Qubit 2.0 fluorometer (Thermo Fisher
394 Scientific) with dsDNA HS Assay Kit reagents (Thermo Fisher Scientific) and the size of the amplicons
395 was controlled on the GX Touch using the 3K kit (X-Mark DNA LabChip, HT DNA NGS 3K Reagent Kit,
396 Perkin Elmer LAS (UK) LTD). Amplicons were pooled equimolarly to 1.5 nM for bacterial and 2.0 nM
397 for fungal libraries according to the molarity. A final 0.7 x magnetic bead clean-up (HighPrep™ PCR
398 Clean-up System, MAGBIO) was performed and the final library pools were eluted in 50 µl EB buffer.

399 **Sequencing on NovaSeq SP flowcell**

400 The libraries were equimolarly pooled for NovaSeq sequencing. Prior to submission the final library
401 pools were concentrated with a 0.7x magnetic bead clean-up and eluted in 50 µl EB buffer. The
402 libraries were sequenced on one SP flow cell on the NovaSeq with a 30 % PhiX spike-in.

403 **Amplicon sequence variant taxonomy assignment and filtering**

404 Amplicon data analysis was conducted as previously described[23,51] with minor alterations: The Illumina
405 binary base call files (bcl) were demultiplexed using bcl2fastq version 2-2.20.0.422 with the settings -
406 -barcode-mismatches 1 --fastq-compression-level 9 into individual fastq.gz files. The paired-end reads
407 were trimmed for primers, sequencing adapters and linker sequences using cutadapt-1.9.1[93] with the
408 settings -n 4 --minimum-length=50. Following cutadapt fastp-0.20.0[94] was run on 16S data with
409 disabled length filter and trim_poly_g to trim polyG read tails. Afterwards both 16S and ITS data was
410 quality controlled, trimmed and filtered using R-3.6.3 and DADA2 version 1.14.1 according to the
411 workflow described in version 2[95]. The truncation length for forward reads was set to 210 bp and the
412 truncation length for the reverse reads to 210 bp for both 16S and ITS. The truncation length was
413 based on read quality. For 16S and ITS libraries we used the following parameters: maxN=0,
414 maxEE=c(2, 2) and truncQ=2 and a minimum length of 50 bp. The filtering parameter maxEE chosen
415 allows for a maximum of 2 expected errors per read, the filtering parameter maxN chosen does not

416 allow any Ns. In addition to filtering using maxEE, maxN and read trimming, a quality score (truncQ)
417 was set that truncates the read at the first nucleotide with a quality score of 2 (set value). After these
418 filtering steps, error rates were estimated as described in[95] and the data was denoised with standard
419 inference settings[95]. Forward and reverse reads were merged with default settings: if the minimum of
420 12 identical bases for overlap was not met between forward and reverse reads, the sample would be
421 omitted. Following the merging of paired reads, a sequence table was constructed with amplicon
422 sequence variants (ASVs). As an additional, subsequent filtering step, chimaeras were removed using
423 standard settings[95]. The Silva (silva_nr99_v138.1.train.set.fa)[96] and UNITE
424 (sh_general_release_dynamic_all_04.04.2024.fasta)[97] databases were then used to taxonomically
425 classify bacterial and fungal reads respectively. Reads that did not match either the bacterial or fungal
426 database were removed.

427 Amplicon sequence variants (ASVs) were used to classify both bacterial and fungal reads. A minimum
428 read number after filtering of 1000 reads per sample and a minimum of three samples per dataset
429 was set as cut-off. We further applied a hard-filter removing all ASVs which were not supported by at
430 least 10 reads per sample and a total relative abundance of 0.1 %. Filtering reduced the number of
431 reads in our 16S libraries from an initial average of 177,387 raw reads to 42,854 reads per library after
432 filtering and assignment to ASVs. For ITS libraries, we initially obtained an average of 77,998 raw reads,
433 which was reduced to 65,666 reads per library following taxonomic assignment. After quality
434 controlling, trimming, taxon assignments and filtering, which were all carried out on the Norwich high-
435 performance computing cluster, we continued with analyses on a desktop machine in R-4.4.1.

436 **Alpha- and beta-diversity comparisons**

437 Alpha-diversity (Shannon and Observed measures) was calculated on pre-normalised data using the
438 phyloseq-1.48.0 package[98]. Statistical significance of diversity differences was assessed with Kruskal-
439 Wallis rank sum tests and pairwise Wilcoxon rank sum tests for non-normally distributed data, or with
440 ANOVA followed by Tukey's HSD for normally distributed data, using default functions in R-4.4.1.

441 For beta-diversity analysis, read counts were transformed using the transform_sample_counts
442 function of phyloseq-1.48.0[98]. Bray-Curtis dissimilarities were calculated with the vegan-2.6 package
443 in R-4.4.1 and community-level differences were tested using ANOSIM and PERMANOVA (adonis
444 function) with the vegan-2.6 package[99]. To visually assess differences between niches we visualised
445 samples using RDA plots in R-4.4.1 and custom ggplot2-3.5.1[83].

446 **Relative abundance plots across niches and conditions**

447 To show relative abundance plots of phyla across plant niches, we used custom R-4.4.1 scrips. We
448 agglomerated taxa to phyla using the phyloseq-1.48.0[98] tax_glom function and visualised relative
449 abundances per phylum as percent-of-all ASVs using ggplot2-3.5.1[83].

450 **Calculating sharedness of ASVs**

451 The sharedness of microbial ASVs between serpentine or non-serpentine populations were calculated
452 using custom R-4.4.1 scripts. ASVs that were found in all each of three serpentine or non-serpentine
453 populations were assigned to the conserved group. ASVs present in two populations were assigned to
454 the shared group. ASVs present in only one population were annotated as unique. The data were
455 visualised using ggplot2-3.5.1[83] in R-4.4.1.

456 **Differential abundance testing of ASVs**

457 Differential abundance (i.e., enrichment) testing between serpentine and non-serpentine conditions
458 for each niche was performed using the default microbiomeMarker-1.10.0[55] settings with its
459 run_limma_voom and marker_table functions in R-4.4.1. Enrichment tables were expanded by
460 connecting ASVs with their taxonomy using custom R-4.4.1 scripts and visualised the data either as a
461 volcano-plot or scatterplots comparing adjusted p-values using custom ggplot2-3.5.1[83]. The
462 comparison between field and transplant enrichment (i.e., log2 fold-change values obtained by the
463 run_limma_voom) function was visualised using ggplot2-3.5.1[83]. Spearman's correlation coefficients
464 were calculated using the stat_cor function of ggpubr-0.6.0[84] in R-4.4.1.

465 **Bray-Curtis comparison of microbiomes**

466 The Bray-Curtis distance of microbiomes from transplanted populations was calculated using the
467 vegdist function of the vegan-2.6 package[99] in R-4.4.1. For each population and niche relative
468 abundance values of genera detected under the serpentine as well as non-serpentine conditions were
469 combined to an abundance matrix. The abundance matrix was analysed using the vegdist function.
470 The obtained results were visualised using custom ggplot2-3.5.1 scripts.

471 **Estimating microbial or genotype variances**

472 To determine genotype profiles of serpentine and non-serpentine populations we compared k-mers
473 of *A. arenosa* genomes previously collected from each population using kWIP-0.2.0[100] default settings.
474 This produced a distance matrix, which was analysed using the default cmdscale function in R-4.4.1.
475 The output of the Classic Multi-dimensional Scaling (MDS) analysis was visualised using ggplot2-
476 3.5.1[83]. This resulted in distinct separation of genotypes by population on the MDS plot.

477 To obtain a single environmental variable describing serpentine versus non-serpentine stress across
478 all tested elements, the previously calculated PC1 values of populations were used. These values
479 captured variation in calcium/magnesium stress and heavy metal composition.

480 To estimate environmental and genotype contributions to bacterial and fungal community assembly,
481 all ASVs that were statistically significantly enriched in the field experiment under either serpentine
482 or non-serpentine conditions were retained. Based on the total relative abundance of each ASV,
483 generalized linear mixed models (GLMMs) were fitted using the glmer function of the lme4-1.1[101]
484 package in R-4.4.1. To disseminate contributions of the genotype or the environment to microbial
485 abundance three models were tested. (1) A full model, in which microbial abundance was explained
486 by both population identity and condition, with time included as a random effect. (2) A population-
487 only model, in which microbial abundance was explained by population identity and time as a random
488 effect. (3) An environment-only model, in which microbial abundance was explained by condition and
489 time as a random effect. All models were fitted using a Gamma distribution with a log link function.
490 Optimization was performed using a maximum number of iterations of 1e5. For each fitted model with
491 a statistically significant contribution of genotype or environment to microbiome assembly,
492 conditional R^2 values were calculated using r2 function of the performance-0.12.4[102] package in R-
493 4.4.1. Model coefficients were extracted and R^2 values visualised using custom ggplot2-3.5.1 scripts.

494

495 **Acknowledgements**

496 We thank Iain Macaulay for helpful discussion about the newest genomic methodologies, Alba
497 Pacheco-Moreno for discussions about plant-microbe interactions and David E. Salt for his support
498 with elemental profiling.

499 **Funding**

500 This work was supported by the European Research Council (ERC) under the European Union's Horizon
501 2020 research and innovation program [grant number ERC-StG 679056 HOTSPOT], via a grant to LY.
502 MG was funded by the BBSRC DTP Studentship Award (BB/M011216/1). MaA was funded by ERC-StG
503 679056 HOTSPOT. JB, MeA and JGM were supported by Biotechnology and Biological Sciences
504 Research Council (BBSRC) Institute Strategic Programme grants BBS/E/J/000PR9797 and
505 BB/X010996/1 to the John Innes Centre. FK and VK were supported by the European Research Council
506 (ERC) under the European Union's Horizon 2020 research and innovation program [grant number ERC-
507 StG 850852 DOUBLE ADAPT], via a grant to FK. ABG was supported by a John Innes Foundation
508 Rotation PhD Studentship.

509 **Data Availability Statement**

510 The sequencing data can be accessed at the NCBI BioProject database (BioProject ID: PRJEB71077).

511 **References**

512 1. Zadel, U. *et al.* Changes induced by heavy metals in the plant-associated microbiome of
513 Miscanthus x giganteus. *Science of The Total Environment* **711**, 134433 (2020).
514 2. Mesa, J. *et al.* Endophytic Cultivable Bacteria of the Metal Bioaccumulator Spartina maritima
515 Improve Plant Growth but Not Metal Uptake in Polluted Marshes Soils. *Front Microbiol* **6**,
516 (2015).
517 3. Feng, N.-X. *et al.* Efficient phytoremediation of organic contaminants in soils using plant–
518 endophyte partnerships. *Science of The Total Environment* **583**, 352–368 (2017).
519 4. Azcón, R., Perálvarez, M. del C., Roldán, A. & Barea, J.-M. Arbuscular mycorrhizal fungi, Bacillus
520 cereus, and Candida parapsilosis from a multicontaminated soil alleviate metal toxicity in
521 plants. *Microb. Ecol.* **59**, 668–677 (2010).
522 5. Gontia-Mishra, I., Sapre, S., Sharma, A. & Tiwari, S. Alleviation of Mercury Toxicity in Wheat by
523 the Interaction of Mercury-Tolerant Plant Growth-Promoting Rhizobacteria. *J Plant Growth*
524 *Regul* **35**, 1000–1012 (2016).
525 6. Schützendübel, A. & Polle, A. Plant responses to abiotic stresses: heavy metal-induced
526 oxidative stress and protection by mycorrhization. *J Exp Bot* **53**, 1351–1365 (2002).
527 7. Cabello-Conejo, M. I. *et al.* Rhizobacterial inoculants can improve nickel phytoextraction by the
528 hyperaccumulator Alyssum pintodasilvae. *Plant Soil* **379**, 35–50 (2014).
529 8. Turner, T. R., James, E. K. & Poole, P. S. The plant microbiome. *Genome Biol.* **14**, 209 (2013).
530 9. Caddell, D. F., Deng, S. & Coleman-Derr, D. Role of the Plant Root Microbiome in Abiotic Stress
531 Tolerance. in *Seed Endophytes: Biology and Biotechnology* (eds. Verma, S. K. & White, J., James
532 Francis) 273–311 (Springer International Publishing, Cham, 2019). doi:10.1007/978-3-030-
533 10504-4_14.
534 10. Schlaeppi, K. & Bulgarelli, D. The Plant Microbiome at Work. *MPMI* **28**, 212–217 (2014).

535 11. Berendsen, R. L., Pieterse, C. M. J. & Bakker, P. A. H. M. The rhizosphere microbiome and plant
536 health. *Trends in Plant Science* **17**, 478–486 (2012).
537 12. Xia, Y., DeBolt, S., Dreyer, J., Scott, D. & Williams, M. A. Characterization of culturable bacterial
538 endophytes and their capacity to promote plant growth from plants grown using organic or
539 conventional practices. *Front Plant Sci* **6**, 490 (2015).
540 13. Schenk, P. M., Carvalhais, L. C. & Kazan, K. Unraveling plant–microbe interactions: can multi-
541 species transcriptomics help? *Trends in Biotechnology* **30**, 177–184 (2012).
542 14. Ritpitakphong, U. *et al.* The microbiome of the leaf surface of Arabidopsis protects against a
543 fungal pathogen. *New Phytol* **210**, 1033–1043 (2016).
544 15. Murphy, B. R., Doohan, F. M. & Hodkinson, T. R. Fungal root endophytes of a wild barley
545 species increase yield in a nutrient-stressed barley cultivar. *Symbiosis* **65**, 1–7 (2015).
546 16. Samad, A., Trognitz, F., Compant, S., Antonielli, L. & Sessitsch, A. Shared and host-specific
547 microbiome diversity and functioning of grapevine and accompanying weed plants. *Environ*
548 *Microbiol* **19**, 1407–1424 (2017).
549 17. Cappelletti, M. *et al.* Leaf Treatments with a Protein-Based Resistance Inducer Partially Modify
550 Phyllosphere Microbial Communities of Grapevine. *Front. Plant Sci.* **7**, (2016).
551 18. Mousa, W. K. *et al.* Root-hair endophyte stacking in finger millet creates a physicochemical
552 barrier to trap the fungal pathogen *Fusarium graminearum*. *Nature Microbiology* **1**, 16167
553 (2016).
554 19. Khalaf, E. M. & Raizada, M. N. Bacterial Seed Endophytes of Domesticated Cucurbits
555 Antagonize Fungal and Oomycete Pathogens Including Powdery Mildew. *Front. Microbiol.* **9**,
556 (2018).
557 20. Kidd, P. S., Álvarez-López, V., Becerra-Castro, C., Cabello-Conejo, M. & Prieto-Fernández, Á.
558 Chapter Three - Potential Role of Plant-Associated Bacteria in Plant Metal Uptake and
559 Implications in Phytotechnologies. in *Advances in Botanical Research* (eds. Cuypers, A. &
560 Vangronsveld, J.) vol. 83 87–126 (Academic Press, 2017).

561 21. Zhalnina, K. *et al.* Dynamic root exudate chemistry and microbial substrate preferences drive
562 patterns in rhizosphere microbial community assembly. *Nat Microbiol* **3**, 470–480 (2018).
563 22. Hu, L. *et al.* Root exudate metabolites drive plant-soil feedbacks on growth and defense by
564 shaping the rhizosphere microbiota. *Nature Communications* **9**, 2738 (2018).
565 23. Pacheco-Moreno, A. *et al.* The genotype of barley cultivars influences multiple aspects of their
566 associated microbiota via differential root exudate secretion. *PLOS Biology* **22**, e3002232
567 (2024).
568 24. Corretto, E. *et al.* Complete genome sequence of the heavy metal resistant bacterium
569 Agromyces aureus AR33T and comparison with related Actinobacteria. *Stand Genomic Sci* **12**,
570 (2017).
571 25. Garaiyurrebaso, O. *et al.* Long-term effects of aided phytostabilisation on microbial
572 communities of metal-contaminated mine soil. *FEMS Microbiol Ecol* **93**, (2017).
573 26. Van Rossum, T. *et al.* Microbiome Analysis Across a Natural Copper Gradient at a Proposed
574 Northern Canadian Mine Site. *Front. Environ. Sci.* **3**, (2016).
575 27. Igwe, A. N. & Vannette, R. L. Bacterial communities differ between plant species and soil type,
576 and differentially influence seedling establishment on serpentine soils. *Plant Soil* (2019)
577 doi:10.1007/s11104-019-04135-5.
578 28. Wójcik, M. *et al.* Chapter One - Metallophytes of Serpentine and Calamine Soils – Their Unique
579 Ecophysiology and Potential for Phytoremediation. in *Advances in Botanical Research* (eds.
580 Cuypers, A. & Vangronsveld, J.) vol. 83 1–42 (Academic Press, 2017).
581 29. Brady, K. U., Kruckeberg, A. R. & Jr, H. D. B. Evolutionary Ecology of Plant Adaptation to
582 Serpentine Soils. *Annual Review of Ecology, Evolution, and Systematics* **36**, 243–266 (2005).
583 30. Bratteler, M., Lexer, C. & Widmer, A. Genetic architecture of traits associated with serpentine
584 adaptation of Silene vulgaris. *Journal of Evolutionary Biology* **19**, 1149–1156 (2006).
585 31. Bothe, H. & Słomka, A. Divergent biology of facultative heavy metal plants. *Journal of Plant*
586 *Physiology* **219**, 45–61 (2017).

587 32. Whittaker, R. H. The Ecology of Serpentine Soils. *Ecology* **35**, 258–288 (1954).

588 33. Arnold, B. J. *et al.* Borrowed alleles and convergence in serpentine adaptation. *Proc. Natl.*
589 *Acad. Sci. U.S.A.* **113**, 8320–8325 (2016).

590 34. Turner, T. L., Bourne, E. C., Von Wettberg, E. J., Hu, T. T. & Nuzhdin, S. V. Population
591 resequencing reveals local adaptation of Arabidopsis lyrata to serpentine soils. *Nat Genet* **42**,
592 260–263 (2010).

593 35. Selby, J. P. & Willis, J. H. Major QTL controls adaptation to serpentine soils in Mimulus guttatus.
594 *Molecular Ecology* **27**, 5073–5087 (2018).

595 36. Sobczyk, M. K., Smith, J. a. C., Pollard, A. J. & Filatov, D. A. Evolution of nickel
596 hyperaccumulation and serpentine adaptation in the Alyssum serpyllifolium species complex.
597 *Heredity* **118**, 31–41 (2017).

598 37. Konečná, V. *et al.* Parallel adaptation in autopolyploid Arabidopsis arenosa is dominated by
599 repeated recruitment of shared alleles. *Nat Commun* **12**, 4979 (2021).

600 38. Konečná, V. *et al.* Genomic basis and phenotypic manifestation of (non-)parallel serpentine
601 adaptation in Arabidopsis arenosa. *Evolution* **76**, 2315–2331 (2022).

602 39. Hassani, M. A., Durán, P. & Hacquard, S. Microbial interactions within the plant holobiont.
603 *Microbiome* **6**, 58 (2018).

604 40. Pascale, A., Proietti, S., Pantelides, I. S. & Stringlis, I. A. Modulation of the Root Microbiome by
605 Plant Molecules: The Basis for Targeted Disease Suppression and Plant Growth Promotion.
606 *Front. Plant Sci.* **10**, (2020).

607 41. Koch, M. A. & Matschinger, M. Evolution and genetic differentiation among relatives of
608 Arabidopsis thaliana. *Proc. Natl. Acad. Sci. U.S.A.* **104**, 6272–6277 (2007).

609 42. Clauss, M. J. & Koch, M. A. Poorly known relatives of Arabidopsis thaliana. *Trends in Plant*
610 *Science* **11**, 449–459 (2006).

611 43. Turisová, I., Štrba, T., Aschenbrenner, Š. & Andráš, P. Arabidopsis arenosa (L.) Law. on
612 metalliferous and non-metalliferous sites in central Slovakia. *Bull Environ Contam Toxicol* **91**,
613 469–474 (2013).
614 44. Preite, V. *et al.* Convergent evolution in Arabidopsis halleri and Arabidopsis arenosa on
615 calamine metalliferous soils. *bioRxiv* 459362 (2018) doi:10.1101/459362.
616 45. Konečná, V., Yant, L. & Kolář, F. The Evolutionary Genomics of Serpentine Adaptation. *Frontiers*
617 *in Plant Science* **11**, (2020).
618 46. Anacker, B. L. The nature of serpentine endemism. *Am. J. Bot.* **101**, 219–224 (2014).
619 47. Veatch-Blohm, M. E., Roche, B. M. & Dahl, E. E. Serpentine populations of Arabidopsis lyrata
620 ssp. lyrata show evidence for local adaptation in response to nickel exposure at germination
621 and during juvenile growth. *Environmental and Experimental Botany* **138**, 1–9 (2017).
622 48. Kazakou, E., Dimitrakopoulos, P. G., Baker, A. J. M., Reeves, R. D. & Troumbis, A. Y. Hypotheses,
623 mechanisms and trade-offs of tolerance and adaptation to serpentine soils: from species to
624 ecosystem level. *Biological Reviews* **83**, 495–508 (2008).
625 49. Main, J. L. Magnesium and Calcium Nutrition of a Serpentine Endemic Grass. *American Midland*
626 *Naturalist* **105**, 196 (1981).
627 50. Rengel, Z., Bose, J., Chen, Q. & Tripathi, B. N. Magnesium alleviates plant toxicity of aluminium
628 and heavy metals. *Crop Pasture Sci.* **66**, 1298 (2015).
629 51. Bollmann-Giolai, A. *et al. A Low-Cost Pipeline for Soil Microbiome Profiling*.
630 http://biorxiv.org/lookup/doi/10.1101/2020.05.07.082305 (2020)
631 doi:10.1101/2020.05.07.082305.
632 52. Malard, L. A. *et al.* Comparative analysis of diversity and environmental niches of soil bacterial,
633 archaeal, fungal and protist communities reveal niche divergences along environmental
634 gradients in the Alps. *Soil Biology and Biochemistry* **169**, 108674 (2022).

635 53. Botha, D. *et al.* Soil type and precipitation level have a greater influence on fungal than
636 bacterial diversity in serpentine and non-serpentine biological soil crusts. *Ecological Research*
637 **39**, 862–878 (2024).
638 54. Escola Oliva, G. *et al.* Rhizosphere microbiome and plant growth promotion bacteria isolates
639 enhance salinity tolerance in salt-sensitive Brassica fruticulosa. (2025)
640 doi:10.22541/au.174124680.05965302/v1.
641 55. Cao, Y. *et al.* microbiomeMarker: an R/Bioconductor package for microbiome marker
642 identification and visualization. *Bioinformatics* **38**, 4027–4029 (2022).
643 56. Akbari, A., Gharanjik, S., Koobaz, P. & Sadeghi, A. Plant growth promoting Streptomyces strains
644 are selectively interacting with the wheat cultivars especially in saline conditions. *Heliyon* **6**,
645 (2020).
646 57. Shepherdson, E. M., Baglio, C. R. & Elliot, M. A. Streptomyces behavior and competition in the
647 natural environment. *Current Opinion in Microbiology* **71**, 102257 (2023).
648 58. Zhang, C. *et al.* Phosphoribosylpyrophosphate synthetase as a metabolic valve advances
649 Methylobacterium/Methylorubrum phyllosphere colonization and plant growth. *Nat Commun*
650 **15**, 5969 (2024).
651 59. Weiß, M. *et al.* Sebacinales Everywhere: Previously Overlooked Ubiquitous Fungal Endophytes.
652 *PLoS ONE* **6**, e16793 (2011).
653 60. Visagie, C. M. *et al.* Identification and nomenclature of the genus *Penicillium*. *Studies in*
654 *Mycology* **78**, 343–371 (2014).
655 61. Lu, X., Cao, T., Nguyễn, T. T. T. & Yuan, H.-S. Six New Species of Tomentella (Thelephorales,
656 Basidiomycota) From Tropical Pine Forests in Central Vietnam. *Front. Microbiol.* **13**, 864198
657 (2022).
658 62. Yang, J. *et al.* Unveiling the Bioactive Compounds and Therapeutic Potential of Russula: A
659 Comprehensive Review. *JoF* **11**, 341 (2025).

660 63. Schechter, S. P. & Bruns, T. D. Edaphic sorting drives arbuscular mycorrhizal fungal community
661 assembly in a serpentine/non-serpentine mosaic landscape. *Ecosphere* **3**, art42 (2012).
662 64. Asif, A., Koner, S., Hussain, B. & Hsu, B.-M. Root-associated functional microbiome endemism
663 facilitates heavy metal resilience and nutrient poor adaptation in native plants under
664 serpentine driven edaphic challenges. *Journal of Environmental Management* **373**, 123826
665 (2025).
666 65. Anderson, H. M. *et al.* Root exudation and rhizosphere microbial assembly are influenced by
667 novel plant trait diversity in carrot genotypes. *Soil Biology and Biochemistry* **197**, 109516
668 (2024).
669 66. Quiza, L. *et al.* The effect of wheat genotype on the microbiome is more evident in roots and
670 varies through time. *ISME COMMUN.* **3**, 32 (2023).
671 67. Yang, P., Zhu, X. & Ning, K. Microbiome-based enrichment pattern mining has enabled a
672 deeper understanding of the biome–species–function relationship. *Commun Biol* **6**, 391 (2023).
673 68. Compant, S., Samad, A., Faist, H. & Sessitsch, A. A review on the plant microbiome: Ecology,
674 functions, and emerging trends in microbial application. *Journal of Advanced Research* **19**, 29–
675 37 (2019).
676 69. Bollmann-Giolai, A. *et al.* A low-cost pipeline for soil microbiome profiling. *Microbiologyopen* **9**,
677 e1133 (2020).
678 70. Bilal, S. *et al.* Endophytic Paecilomyces formosus LHL10 Augments Glycine max L. Adaptation to
679 Ni-Contamination through Affecting Endogenous Phytohormones and Oxidative Stress. *Front.*
680 *Plant Sci.* **8**, 870 (2017).
681 71. Surono & Narisawa, K. The dark septate endophytic fungus Phialocephala fortinii is a potential
682 decomposer of soil organic compounds and a promoter of Asparagus officinalis growth. *Fungal*
683 *Ecology* **28**, 1–10 (2017).
684 72. Branco, S. & Ree, R. H. Serpentine Soils Do Not Limit Mycorrhizal Fungal Diversity. *PLOS ONE* **5**,
685 e11757 (2010).

686 73. Panaccione, D. G., Sheets, N. L., Miller, S. P. & Cumming, J. R. Diversity of Cenococcum
687 geophilum isolates from serpentine and non-serpentine soils. *Mycologia* **93**, 645–652 (2001).
688 74. Santoyo, G. How plants recruit their microbiome? New insights into beneficial interactions.
689 *Journal of Advanced Research* **40**, 45–58 (2022).
690 75. Oyserman, B. O. *et al.* Extracting the GEMs: Genotype, Environment, and Microbiome
691 Interactions Shaping Host Phenotypes. *Front. Microbiol.* **11**, (2021).
692 76. Petersen, C. *et al.* Host and microbiome jointly contribute to environmental adaptation. *ISME J*
693 **17**, 1953–1965 (2023).
694 77. Bhar, A., Chakraborty, A. & Roy, A. The captivating role of calcium in plant-microbe interaction.
695 *Front. Plant Sci.* **14**, 1138252 (2023).
696 78. Coleman-Derr, D. & Tringe, S. G. Building the crops of tomorrow: advantages of symbiont-
697 based approaches to improving abiotic stress tolerance. *Front. Microbiol.* **5**, (2014).
698 79. Bollmann-Giolai, A., Malone, J. G. & Arora, S. Diversity, detection and exploitation: linking soil
699 fungi and plant disease. *Current Opinion in Microbiology* **70**, 102199 (2022).
700 80. Dombrowski, N. *et al.* Root microbiota dynamics of perennial Arabis alpina are dependent on
701 soil residence time but independent of flowering time., Root microbiota dynamics of perennial
702 Arabis alpina are dependent on soil residence time but independent of flowering time. *ISME J*
703 **11, 11**, 43, 43–55 (2017).
704 81. Copeland, J. K., Yuan, L., Layeghifard, M., Wang, P. W. & Guttman, D. S. Seasonal Community
705 Succession of the Phyllosphere Microbiome. *MPMI* **28**, 274–285 (2015).
706 82. Danku, J. M. C., Lahner, B., Yakubova, E. & Salt, D. E. Large-Scale Plant Ionomics. in *Plant*
707 *Mineral Nutrients: Methods and Protocols* (ed. Maathuis, F. J. M.) 255–276 (Humana Press,
708 Totowa, NJ, 2013). doi:10.1007/978-1-62703-152-3_17.
709 83. Ginestet, C. ggplot2: Elegant Graphics for Data Analysis. *Journal of the Royal Statistical Society:*
710 *Series A (Statistics in Society)* **174**, 245–246 (2011).

711 84. Kassambara, A. ggpubr: ‘ggplot2’ Based Publication Ready Plots. 0.6.1
712 https://doi.org/10.32614/CRAN.package.ggpubr (2016).
713 85. Kassambara, A. & Mundt, F. factoextra: Extract and Visualize the Results of Multivariate Data
714 Analyses. 1.0.7 https://doi.org/10.32614/CRAN.package.factoextra (2016).
715 86. Massicotte, P. & South, A. rnaturalearth: World Map Data from Natural Earth. 1.1.0
716 https://doi.org/10.32614/CRAN.package.rnaturalearth (2017).
717 87. Bulgarelli, D. *et al.* Revealing structure and assembly cues for Arabidopsis root-inhabiting
718 bacterial microbiota. *Nature* **488**, 91–95 (2012).
719 88. Bodenhausen, N., Horton, M. W. & Bergelson, J. Bacterial communities associated with the
720 leaves and the roots of Arabidopsis thaliana. *PLoS ONE* **8**, e56329 (2013).
721 89. Horton, M. W. *et al.* Genome-wide association study of Arabidopsis thaliana leaf microbial
722 community. *Nat Commun* **5**, 5320 (2014).
723 90. Qvit-Raz, N., Jurkevitch, E. & Belkin, S. Drop-size soda lakes: transient microbial habitats on a
724 salt-secreting desert tree. *Genetics* **178**, 1615–1622 (2008).
725 91. Walters, W. *et al.* Improved Bacterial 16S rRNA Gene (V4 and V4-5) and Fungal Internal
726 Transcribed Spacer Marker Gene Primers for Microbial Community Surveys. *mSystems* **1**,
727 e00009-15 (2016).
728 92. Lundberg, D. S., Yourstone, S., Mieczkowski, P., Jones, C. D. & Dangl, J. L. Practical innovations
729 for high-throughput amplicon sequencing. *Nat Meth* **10**, 999–1002 (2013).
730 93. Martin, M. Cutadapt removes adapter sequences from high-throughput sequencing reads.
731 *EMBnet.journal* **17**, 10–12 (2011).
732 94. Chen, S., Zhou, Y., Chen, Y. & Gu, J. fastp: an ultra-fast all-in-one FASTQ preprocessor.
733 *Bioinformatics* **34**, i884–i890 (2018).
734 95. Callahan, B. J., Sankaran, K., Fukuyama, J. A., McMurdie, P. J. & Holmes, S. P. Bioconductor
735 Workflow for Microbiome Data Analysis: from raw reads to community analyses.
736 *F1000Research* **5**, 1492 (2016).

96. Quast, C. *et al.* The SILVA ribosomal RNA gene database project: improved data processing and web-based tools. *Nucleic Acids Res* **41**, D590–D596 (2013).

97. Nilsson, R. H. *et al.* The UNITE database for molecular identification of fungi: handling dark taxa and parallel taxonomic classifications. *Nucleic Acids Res* **47**, D259–D264 (2019).

98. McMurdie, P. J. & Holmes, S. phyloseq: An R Package for Reproducible Interactive Analysis and Graphics of Microbiome Census Data. *PLOS ONE* **8**, e61217 (2013).

99. Dixon, P. VEGAN, a package of R functions for community ecology. *Journal of Vegetation Science* **14**, 927–930 (2003).

100. Murray, K. D., Webers, C., Ong, C. S., Borevitz, J. & Warthmann, N. kWIP: The k-mer weighted inner product, a de novo estimator of genetic similarity. *PLoS Comput Biol* **13**, e1005727 (2017).

101. Bates, D., Maechler, M., Bolker, B. & Walker, S. lme4: Linear Mixed-Effects Models using 'Eigen' and S4. 1.1-37 https://doi.org/10.32614/CRAN.package.lme4 (2003).

102. Lüdecke, D. *et al.* performance: Assessment of Regression Models Performance. 0.15.0 https://doi.org/10.32614/CRAN.package.performance (2019).

754 **Figures**

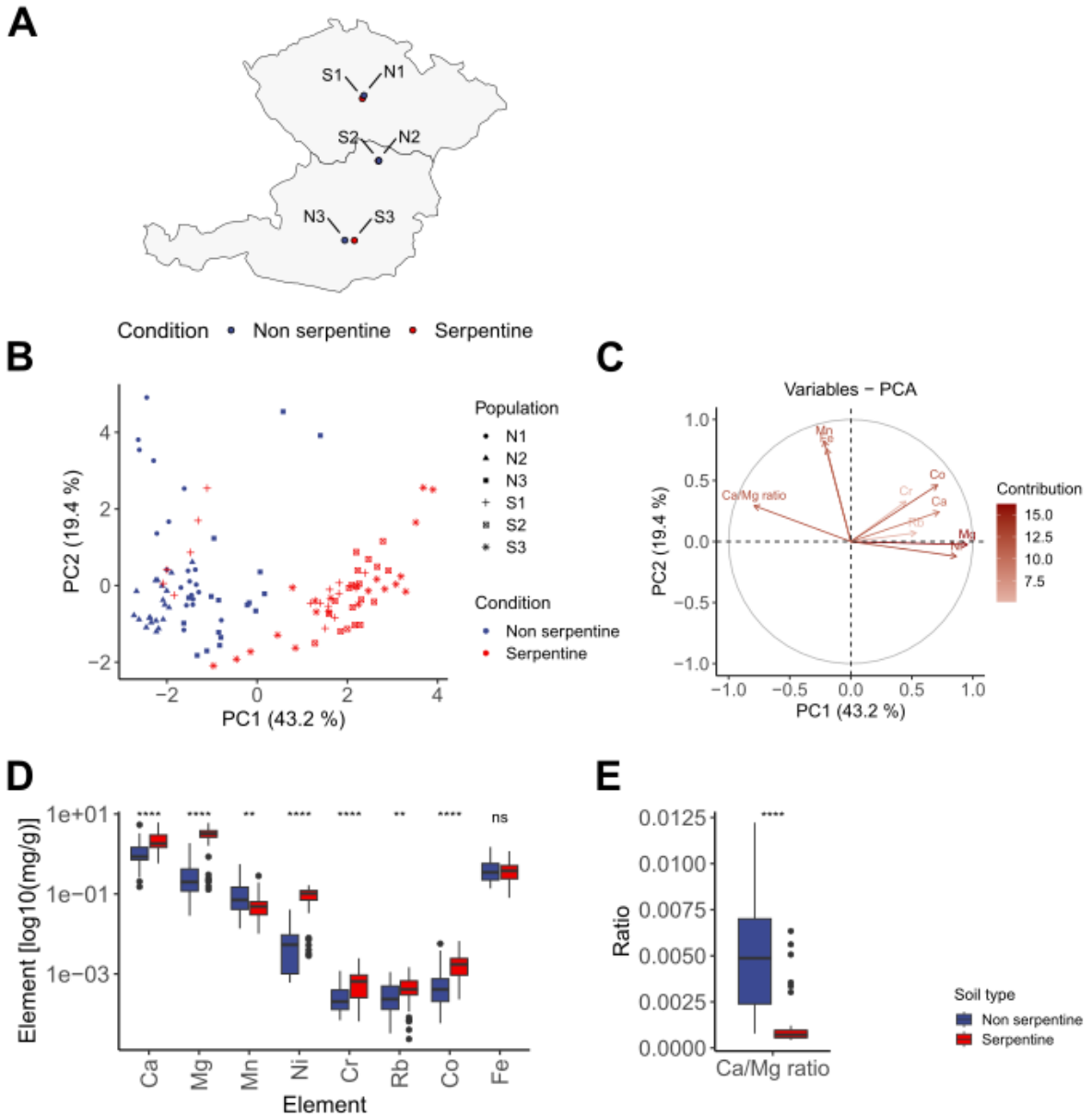

755

756 **Fig. 1 Serpentine soils, and their associated *A. arenosa* populations, display elevated metal ion**
757 **concentrations and a lower calcium to magnesium ratio than non-serpentine samples. (A)**
758 Geographical locations of serpentine and non-serpentine populations in Austria and the Czech
759 Republic. **(B)** PCA of soil ion composition showing clear separation of serpentine and non-serpentine
760 sites. **(C)** PCA biplot illustrating contributions of individual ions and the Ca/Mg ratio to the first two
761 principal components. **(D)** Ion concentrations obtained from soil profiling. Labels indicate statistically
762 significant differences between serpentine and non-serpentine soils (t-test).
763 **(E)** Difference in Ca/Mg ratio between serpentine and non-serpentine soils (t-test). ($p < 0.0001$****, p
764 < 0.001***, $p < 0.01$**, $p < 0.05$*; not significant: ns)

765

766

767

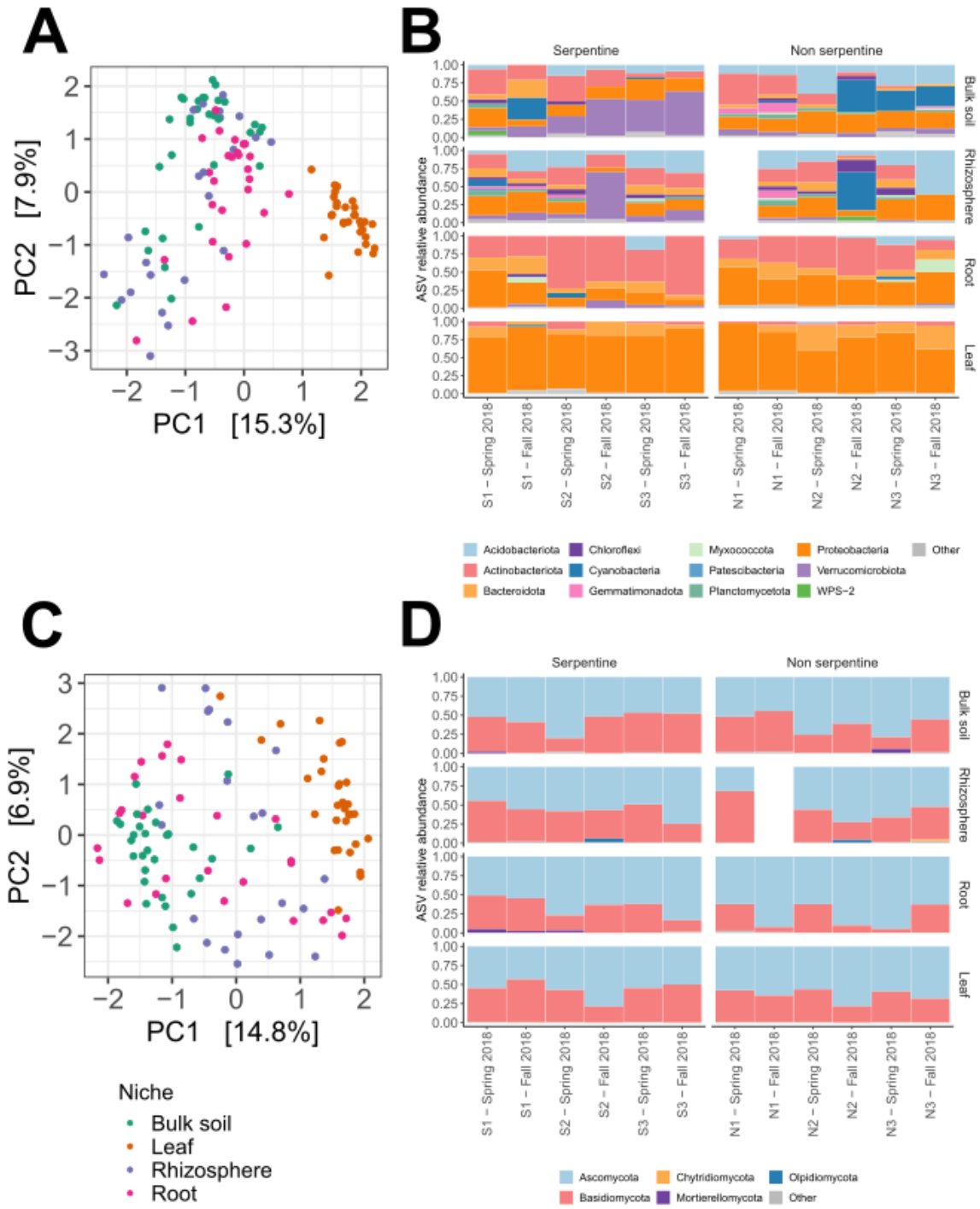

Fig. 2 Higher bacterial variation in below-ground niches and higher uniformity for fungal communities across all niches. (A) RDA of bacterial communities in bulk soil, rhizosphere, root, and leaf niches. **(B)** Relative abundance of bacterial phyla across all populations and seasons (spring and fall 2018). **(C)** RDA of fungal communities in bulk soil, rhizosphere, root, and leaf niches. **(D)** Relative abundance of fungal phyla across all populations and seasons (spring and fall 2018). Fall 2018 was used as representative season for A and C. (Phyla with a total relative abundance of less than 2 % were grouped as 'Other'.)

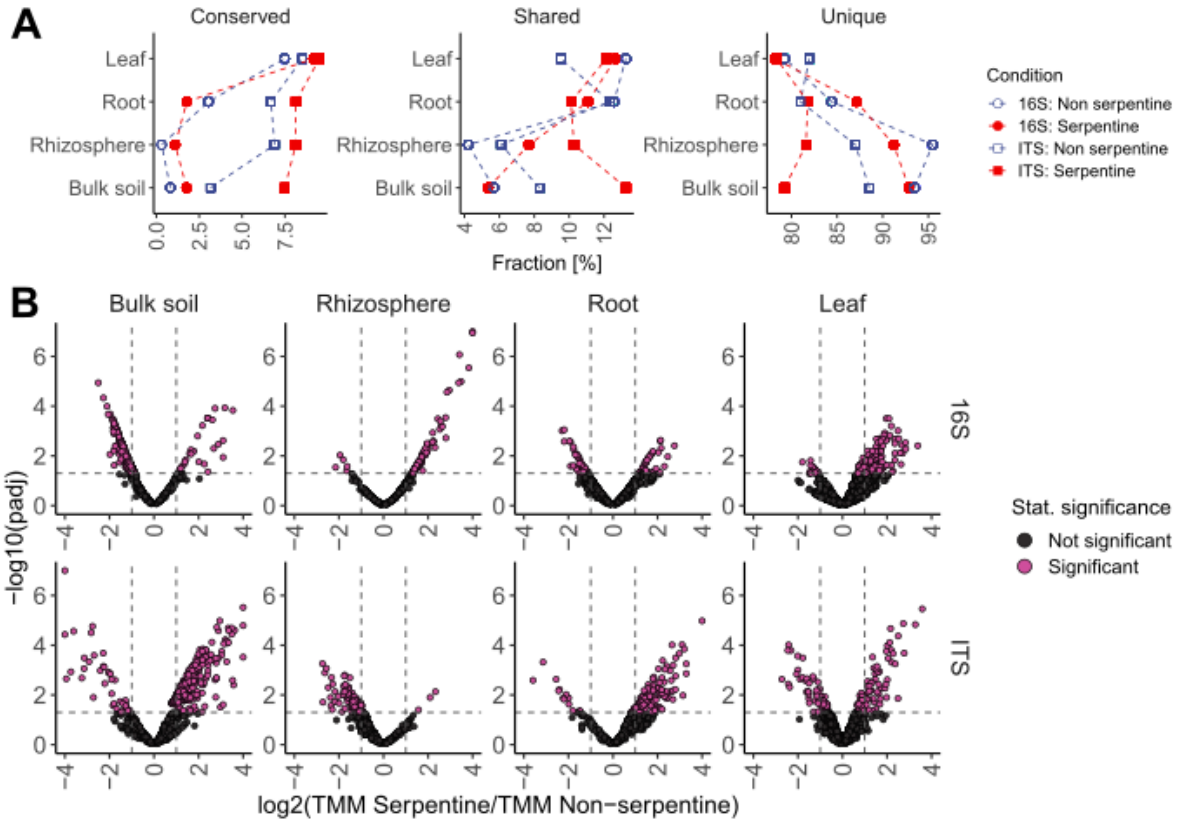

Fig. 3 Similarity of bacterial and fungal microbiomes across plant populations based on ASV presence-absence and differential enrichment. (A) Distribution of bacterial and fungal ASVs across niches, categorised as conserved (present in all three populations), shared (present in two populations), or unique (restricted to a single population). Fungal ASVs were more conserved than bacterial ASVs under both serpentine and non-serpentine conditions. **(B)** Differential abundance of conserved bacterial and fungal ASVs between serpentine and non-serpentine soils. Volcano plots show significantly enriched ASVs.

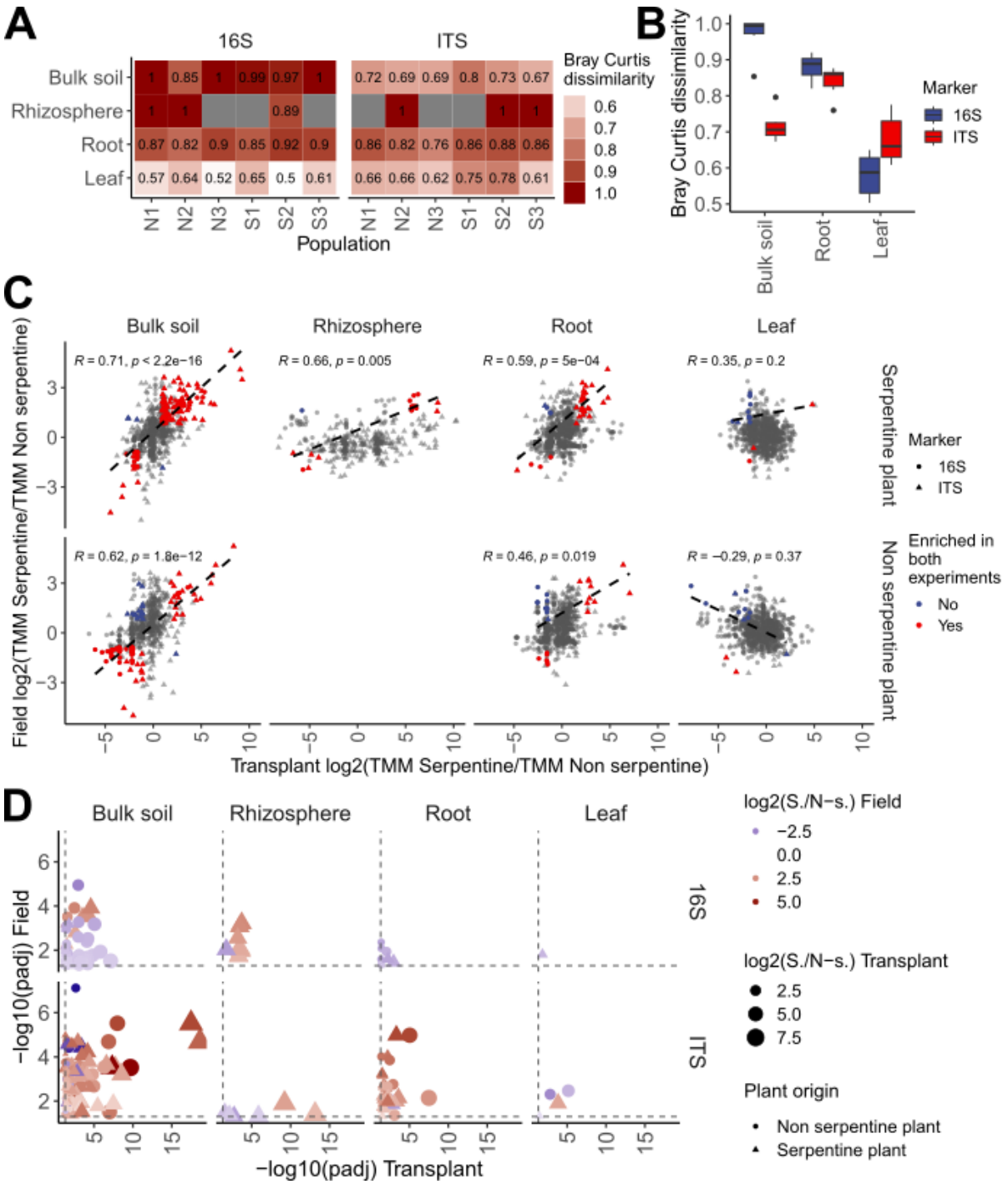

Fig. 4 Microbiome responses in a reciprocal transplant experiment. (A,B) Bray-Curtis dissimilarity shows that microbiomes of transplanted plants differ from, but partially retain, those in native soils, with fungi showing greater similarity across compartments than bacteria. The heatmap in **(A)** shows Bray-Curtis dissimilarity scores per population and niche for bacteria and fungi, boxplot **(B)** visualises the Bray-Curtis dissimilarity scores next to one another across niches. **(C)** Spearman correlations of log2 fold-changes reveal that serpentine plants more closely mirror field enrichment patterns than non-serpentine plants, particularly belowground. **(D)** Differential abundance analysis identifies ASVs enriched in serpentine versus non-serpentine soils, with overlap to field-enriched ASVs highlighting candidates potentially contributing to serpentine adaptation.

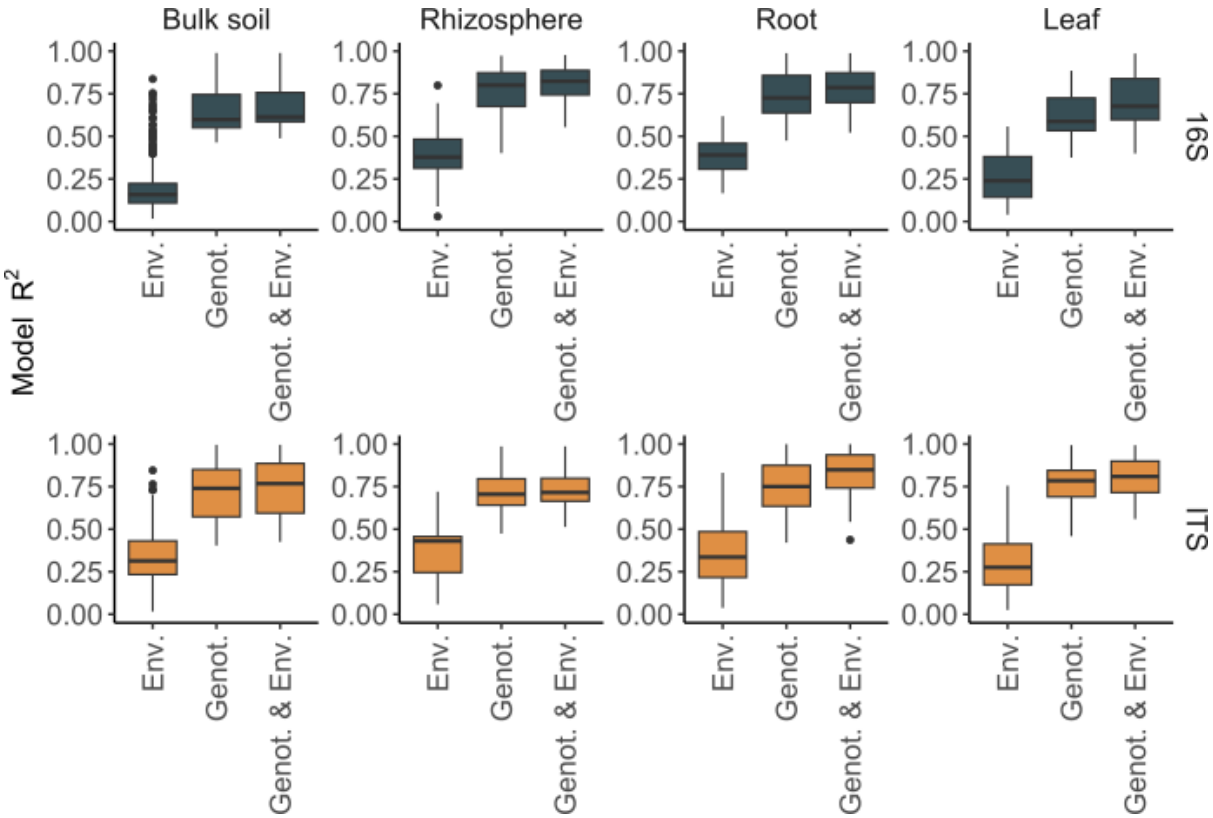

Fig. 5 Contributions of genotype and environment to microbiome composition. Explained variance (R^2) of ASV abundance is shown for statistically significant models predicting ASV relative abundance, with genotype and environment as fixed factors and time as a random factor. While the combination of genotype and environment best predicts ASV abundance, genetic effects consistently exceed environmental effects in shaping microbiome assembly.

Additional Files

Extended Data File 1: Statistical analysis of ion compositions in serpentine and non-serpentine soils.

Extended Data File 2: Word document containing supplementary figures, alpha- and beta-diversity analyses.

Extended Data File 3: Percentages of bacterial and fungal phyla detected across seasons, populations, and niches.

Extended Data File 4: Percentages of conserved, shared, and unique fungal and bacterial ASVs across populations.

Extended Data File 5: Table displaying percentages of bacterial and fungal ASVs enriched in serpentine and non-serpentine soils.

Extended Data File 6: Results from field enrichment testing.

Extended Data File 7: ASVs per genus from the field enrichment experiment.

Extended Data File 8: Comparison of transplant and field enrichment testing results.

Extended Data File 9: Overlap of enrichment testing for serpentine-enriched bacterial and fungal ASVs between field and transplant.

Extended Data File 10: Excel file containing sequencing adapters, barcodes, and primers.

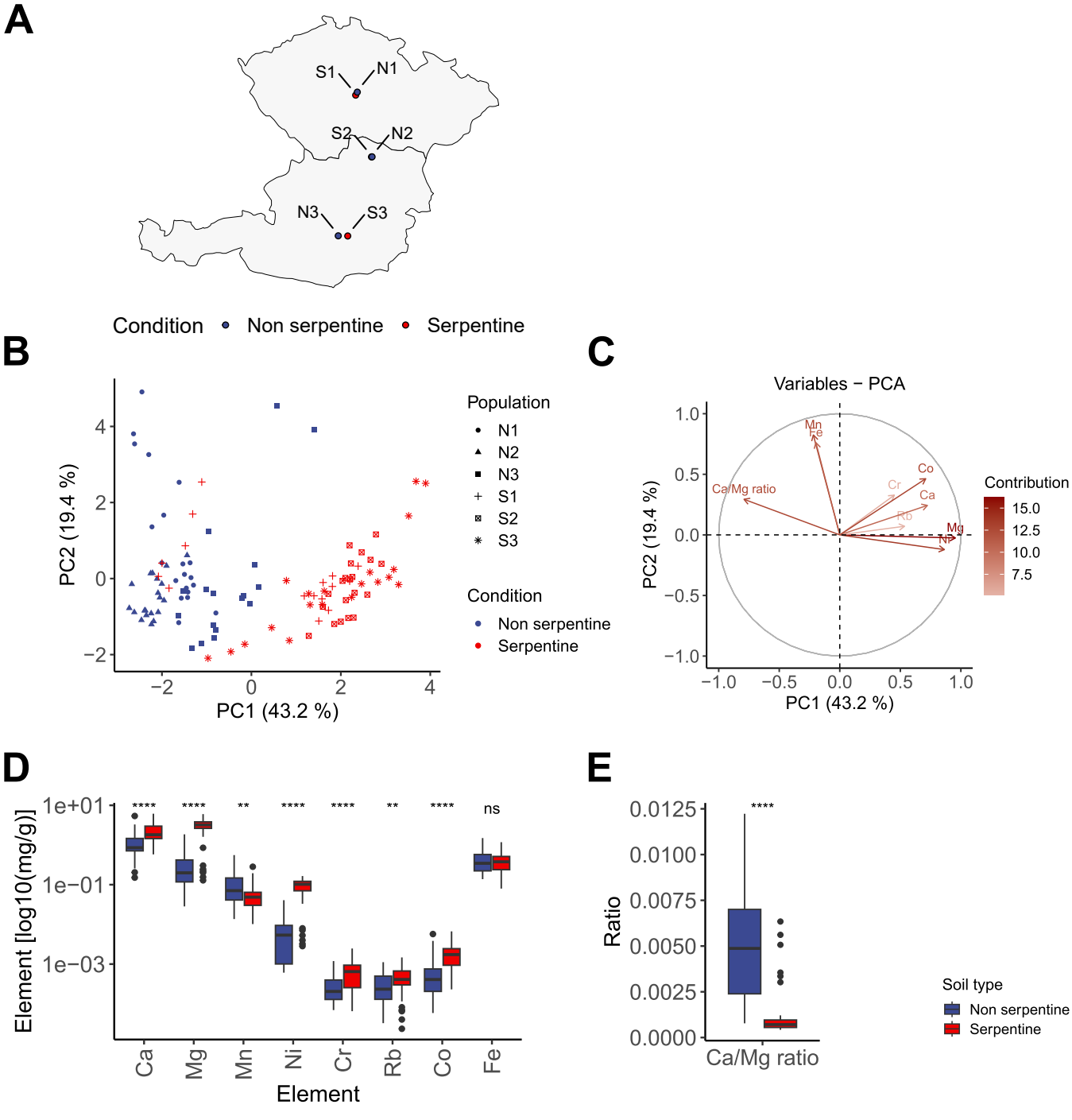
A
S1
N1
S2
N2
N3
S3
Condition
Non serpentine
Serpentine
B
PC2 (19.4 %)
PC1 (43.2 %)
Population
N1
N2
N3
S1
S2
S3
Condition
Non serpentine
Serpentine
C
Variables − PCA
PC2 (19.4 %)
PC1 (43.2 %)
Mn
Fe
Co
Cr
Ca
Rb
Mg
Ni
Ca/Mg ratio
Contribution
15.0
12.5
10.0
7.5
D
Element [log10(mg/g)]
1e+01
1e−01
1e−03
****
****
**
****
****
**
****
ns
Ca
Mg
Mn
Ni
Cr
Rb
Co
Fe
Element
E
Ratio
0.0125
0.0100
0.0075
0.0050
0.0025
0.0000
****
Ca/Mg ratio
Soil type
Non serpentine
Serpentine

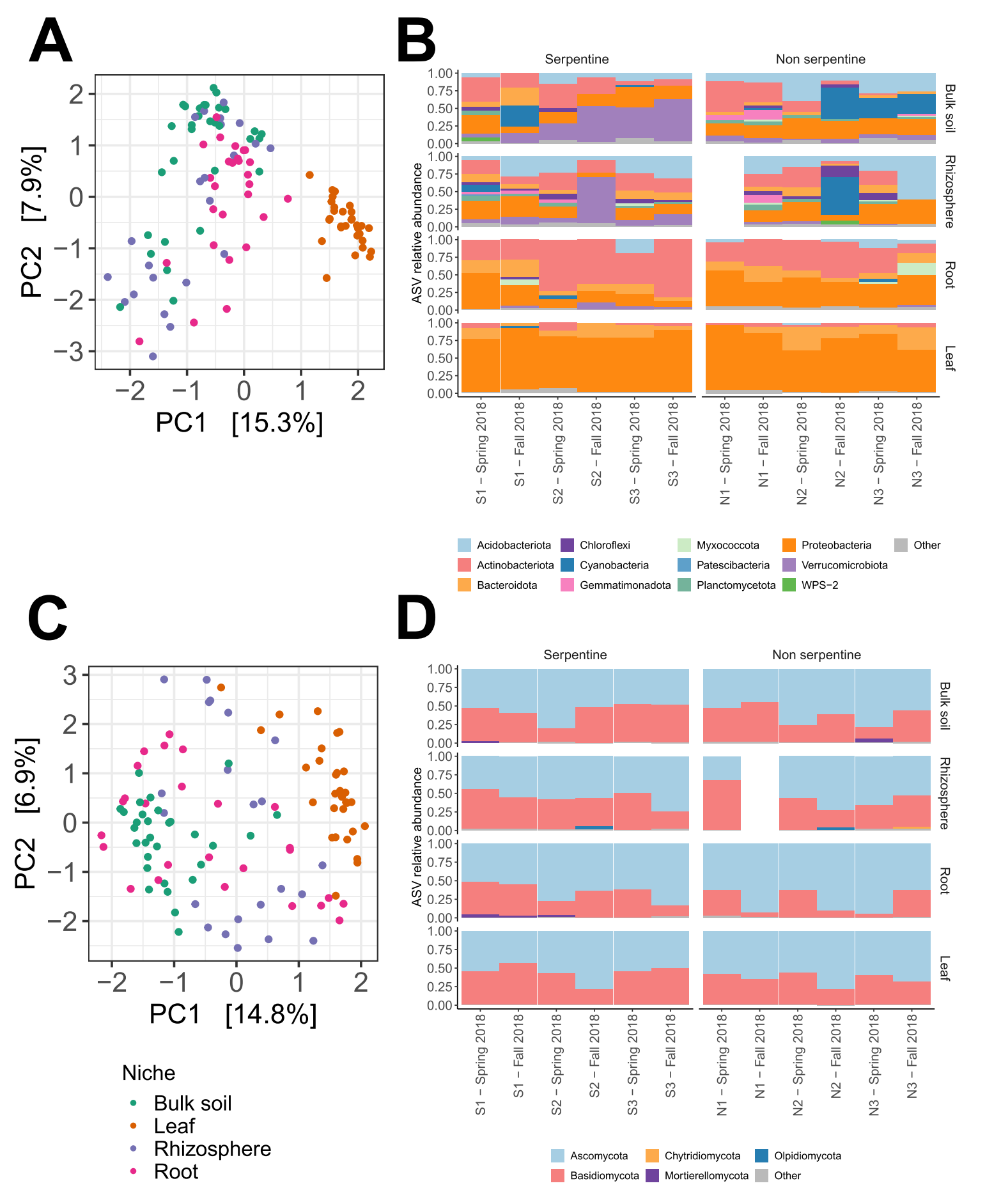
A
PC2 [7.9%]
PC1 [15.3%]
B
Serpentine
Non serpentine
Bulk soil
Rhizosphere
Root
Leaf
ASV relative abundance
S1 – Spring 2018
S1 – Fall 2018
S2 – Spring 2018
S2 – Fall 2018
S3 – Spring 2018
S3 – Fall 2018
N1 – Spring 2018
N1 – Fall 2018
N2 – Spring 2018
N2 – Fall 2018
N3 – Spring 2018
N3 – Fall 2018
Acidobacteriota
Actinobacteriota
Bacteroidota
Chloroflexi
Cyanobacteria
Gemmatimonadota
Myxococcota
Patescibacteria
Planctomycetota
Proteobacteria
Verrucomicrobiota
WPS−2
Other
C
PC2 [6.9%]
PC1 [14.8%]
Niche
Bulk soil
Leaf
Rhizosphere
Root
D
Serpentine
Non serpentine
Bulk soil
Rhizosphere
Root
Leaf
ASV relative abundance
Ascomycota
Basidiomycota
Chytridiomycota
Mortierellomycota
Olpidiomycota
Other

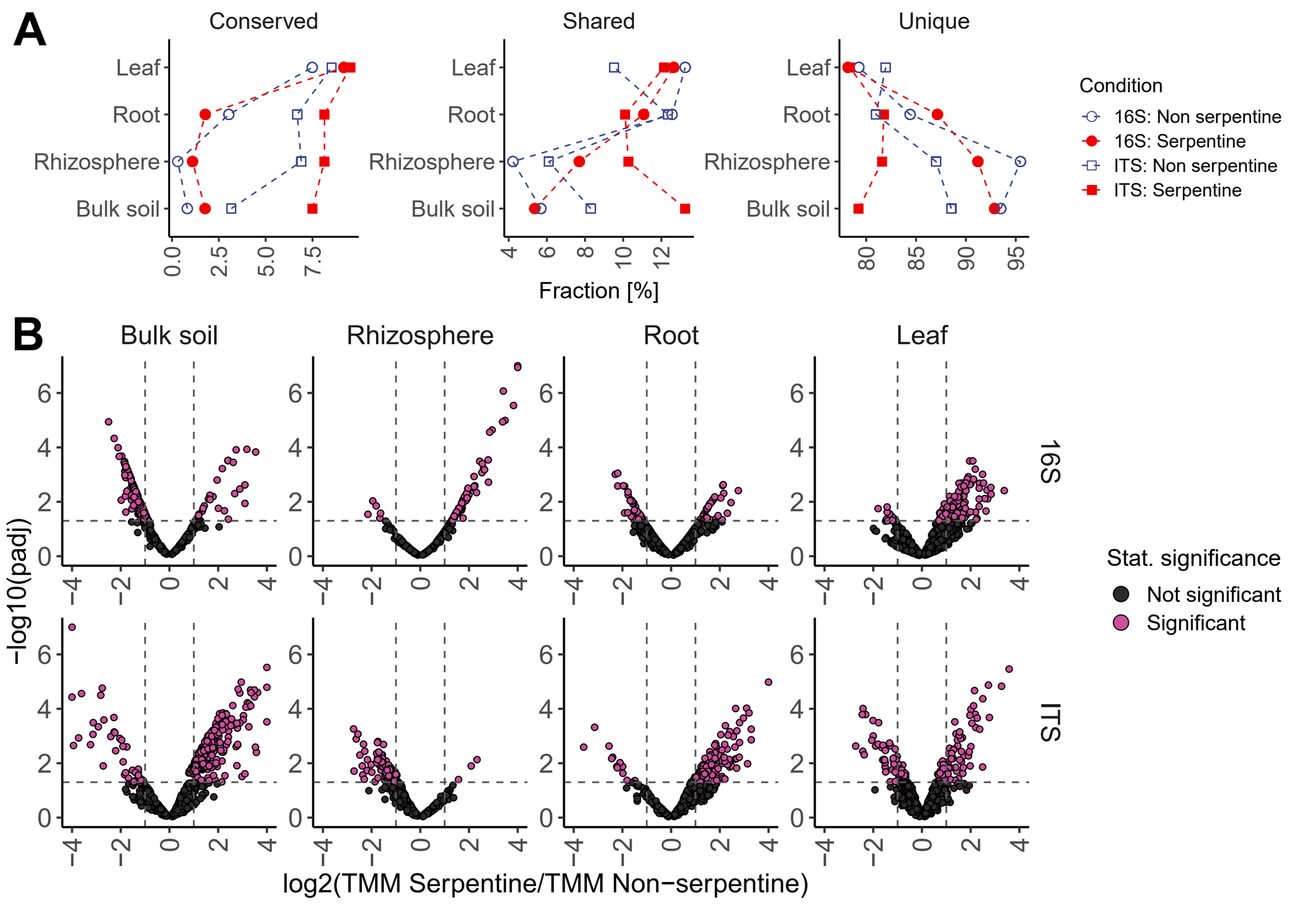
A
Conserved
Shared
Unique
Leaf
Root
Rhizosphere
Bulk soil
0.0
2.5
5.0
7.5
4
6
8
10
12
80
85
90
95
Fraction [%]
Condition
16S: Non serpentine
16S: Serpentine
ITS: Non serpentine
ITS: Serpentine
B
Bulk soil
Rhizosphere
Root
Leaf
16S
ITS
−log10(padj)
log2(TMM Serpentine/TMM Non−serpentine)
Stat. significance
Not significant
Significant

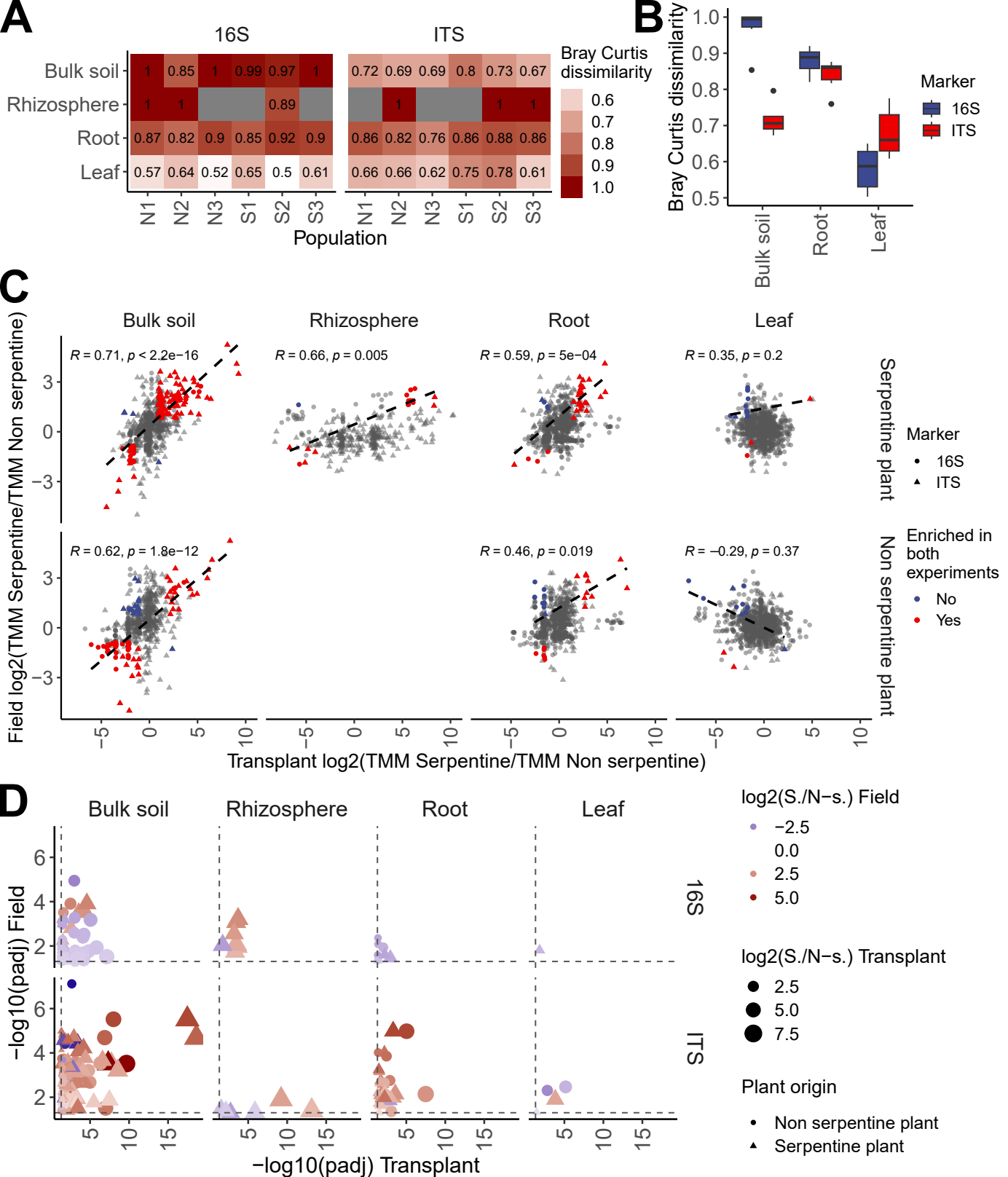
A
16S
ITS
Bulk soil
Rhizosphere
Root
Leaf
1 0.85 1 0.99 0.97 1
1 1 0.89
0.87 0.82 0.9 0.85 0.92 0.9
0.57 0.64 0.52 0.65 0.5 0.61
0.72 0.69 0.69 0.8 0.73 0.67
1 1 1
0.86 0.82 0.76 0.86 0.88 0.86
0.66 0.66 0.62 0.75 0.78 0.61
N1 N2 N3 S1 S2 S3
Population
Bray Curtis dissimilarity
0.6
0.7
0.8
0.9
1.0
B
Bray Curtis dissimilarity
Marker
16S
ITS
Bulk soil
Root
Leaf
C
Bulk soil
Rhizosphere
Root
Leaf
R = 0.71, p < 2.2e−16
R = 0.66, p = 0.005
R = 0.59, p = 5e−04
R = 0.35, p = 0.2
R = 0.62, p = 1.8e−12
R = 0.46, p = 0.019
R = −0.29, p = 0.37
Serpentine plant
Non serpentine plant
Field log2(TMM Serpentine/TMM Non serpentine)
Transplant log2(TMM Serpentine/TMM Non serpentine)
Marker
16S
ITS
Enriched in both experiments
No
Yes
D
Bulk soil
Rhizosphere
Root
Leaf
16S
ITS
−log10(padj) Field
−log10(padj) Transplant
log2(S./N−s.) Field
−2.5
0.0
2.5
5.0
log2(S./N−s.) Transplant
2.5
5.0
7.5
Plant origin
Non serpentine plant
Serpentine plant

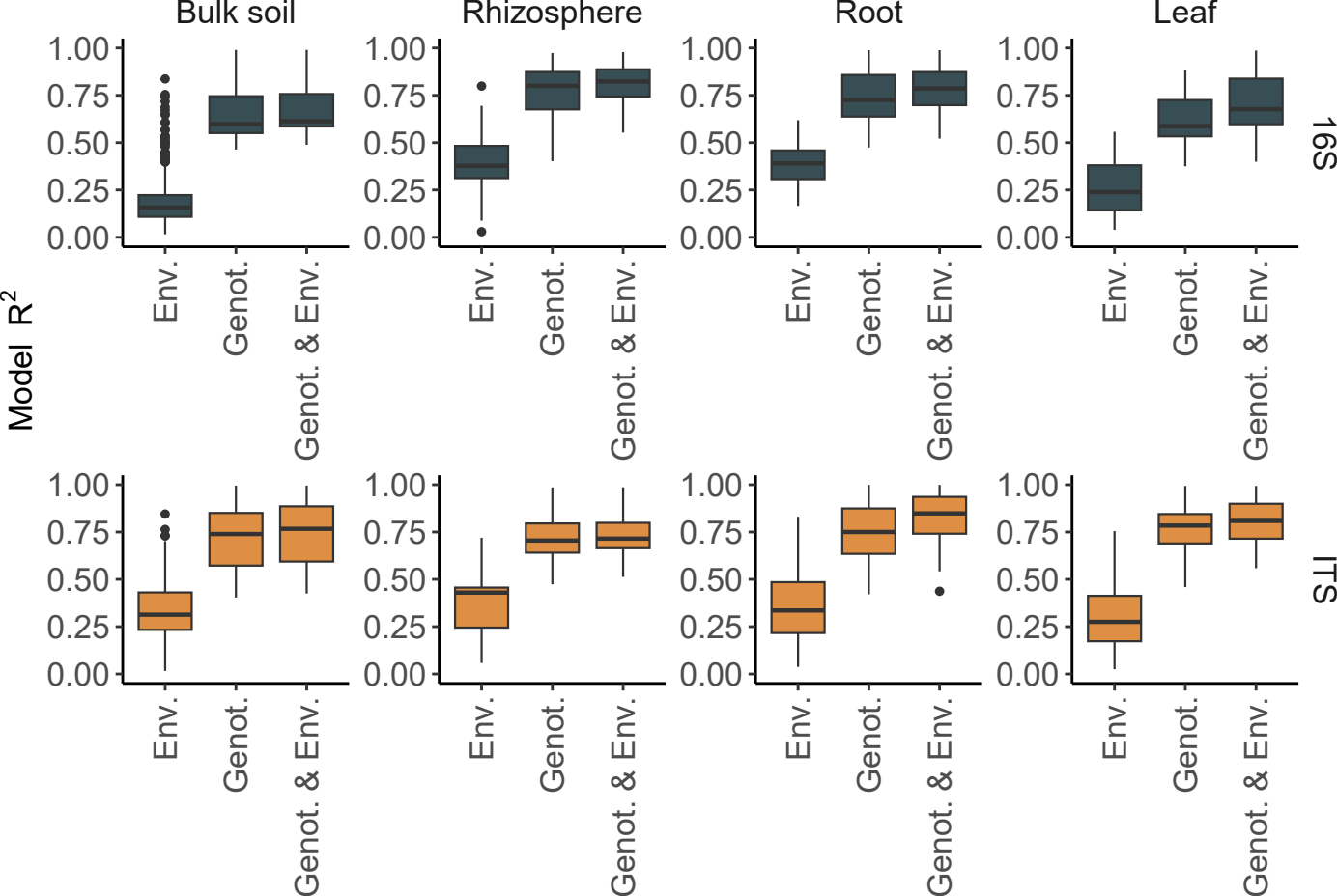
Bulk soil
Rhizosphere
Root
Leaf
16S
ITS
Model R^2
1.00
0.75
0.50
0.25
0.00
Env.
Genot.
Genot. & Env.